TECHNICAL UNIVERSITY OF LIBEREC
Faculty of Textile Engineering

Knife Stabbing Resistance of Woven Fabrics

Muhammad Usman Javaid, MIT

SUMMARY OF THE THESIS

Title of the thesis:	Knife Stabbing Resistance of Woven Fabrics
Author:	Muhammad Usman Javaid
Field of study:	Textile Technics and Materials Engineering
Mode of study:	Part time
Department:	Department of Material Engineering
Supervisor:	Ing. Jana Salačová

Committee for defense of the dissertation:

Chairman:	
prof. Dr. Ing. Zdeněk Kůs	FT TUL, katedra oděvnictví
Vice-chairman:	
doc. Ing. Vladimír Bajzík, Ph.D.	FT TUL, katedra hodnocení textilií
prof. Ing. Michal Šejnoha, Ph.D., DSc. (oponent)	Fakulta stavební ČVUT, katedra mechaniky
prof. Ing. Miroslav Václavík, CSc.	VÚTS a.s.
doc. Ing. Lukáš Čapek, Ph.D. (oponent)	FT TUL, katedra technologií a struktur
doc. Ing. Rajesh Mishra, Ph.D, B.Tech.	FT TUL, katedra materiálového inženýrství
Ing. Petr Henyš, Ph.D.	FT TUL, katedra technologií a struktur
Ing. Brigita Kolčavová Sirková, Ph.D.	FT TUL, katedra technologií a struktur
Ing. Blanka Tomková, Ph.D.	FT TUL, katedra materiálového inženýrství

The dissertation is available at the Dean's Office FT TUL.

Liberec 2019

ABSTRACT

This research focused on the stabbing response of woven fabrics. Woven fabric investigated in this work had an equal set of warp and weft Twaron® para-Aramid filament yarns. In this work, isotropy of single sheet and multiple-sheets stacked together was analyzed at different orientations of knife stabbing. During knife stabbing a knife penetration angle (KPA) is formed between the knife cutting axis and warp yarn of the fabric. The study was conducted at five different cutting angles i.e. 0°, 22.5°, 45°, 67.5°, and 90°. Quasi-static knife penetration resistance (QSKPR) and dynamic stab resistance (DSR) of the woven fabrics were studied in this work.

The main objective of this research was to study the behavior of dry woven fabrics whose surface was modified to change their friction. The selection and application of these modifications were made in such a way to keep the comfort and flexibility characteristics minimally affected. We adopted three surface modification techniques; 1) SiO_2 deposition, 2) Ozone treatment along with SiO_2 deposition and 3) TiO_2 deposition. Furthermore, the effect of treatment was characterized against surface topology, anti-stabbing behavior, mechanical, comfort and friction properties of developed fabrics.

This research discovered a new method of SiO_2 deposition, using Water Glass (WG) as a precursor. The deposition of SiO_2 was investigated and confirmed using Scanning Electron Microscopy (SEM), Fourier Transfer Infra-Red (FTIR) spectroscopy, and Energy-Dispersive X-ray (EDX) spectroscopy. The concentration of WG showed the direct relation for an increase in QSKPR. At 40% solution of WG the QSKPR was observed about 200%.

The QSKPR measured at 67.5° KPA for untreated fabric was found statistically significantly higher than the mean QSKPR measured for all KPAs. Moreover, the QSKPR seems to follow a specific pattern for different KPAs, irrespective of fabric treatment.

The coefficient of friction of fabric surface was well improved by the deposition layer of SiO_2. Hence, the yarn pull-out force was increased for treated fabrics as compared to untreated. It was also observed that, treatment with Ozone before depositing SiO_2, reduces the adverse effect on comfort and flexibility characteristics of fabric.

The quasi-static stabbing was found to be the complementary response to warp and weft yarns, due to their orthogonal orientation. This response was modelled with the Fourier function, that fits well to the quasi-static stab of different fabrics. It was also observed that the behaviour of this response is directly proportional to fabric's coefficient of friction and inversely proportional to the gap between yarns.

The interaction of the knife and the fabric was recorded on CCD camera, during QSKPR measurements. It was observed that the shape of the knife profile plays a major role. The blunt edge of the knife finds maximum resistance and causes the major peak in the force-displacement curve. While after the complete penetration of blunt edge, individual yarns cut one by one. It is proposed that SiO_2 deposition increases inter-fiber friction, as a result the filaments of the yarn behave as single assembly rather as individual filament against the sharp edge of the knife.

Yarn sliding resistance, individual yarn cutting behaviour and yarn pull out force was measured for warp and weft directions of treated and untreated fabrics. It was found that the major response of stabbing resistance depends upon inter yarn friction, while intra-yarn friction accounts for penetration energy of individual yarn.

QSKPR was measured for two sheets, oriented at three stacking angles (SA). The 45° SA was found to exhibit better response of QSKPR than 0°and 90° SA. A modified version of NIJ standard–0115.00 was followed to verify the dynamic stab resistance at 45° SA. It was found that 45° SA exhibits isotropic stab resistance in all KPAs. Furthermore, treated fabrics showed 200% higher stab resistance than untreated fabrics.

Keywords: Stab Resistance; Silicon dioxide; Titanium dioxide; Ozone; Aramid; Woven; Sodium Silicate; Water Glass

Abstrakt

Tato práce je zaměřena konstrukci a hodnocení vlastností vrstvených textilních struktur s zvýšenou odolností proti pronikání nožů. Každá vrstva je tkaná textilie vyrobená z para-aramidového vlákna Twaron® se stejnou dostavou ve směru osnovy a útku. Je analyzována anizotropie odporu proti pronikání nože jedné i vice vrstev tkaniny. Orientace odporu proti pronikání je charakterizována úhlem penetrace nože (KPA) mezi osou řezání nožem a směrem osnovy tkaniny. Tento úhel byl měněn v pěti směrech řezu, tedy 0°; 22,5°; 45°; 67,5° a 90°. Byla zkoumána kvazi-statická odolnost proti pronikání nože (QSKPR) a dynamická odolnost proti pronikání nože (DSR) tkaninou.

Základním cílem této práce je úprava povrchu vláken tak, aby se změnily jejich třecí vlastnosti. Výběr a aplikaci těchto úprav je třeba provést tak, aby nebyly negativně ovlivněny vlastnosti charakterizující komfort. Ze tří předběžně vytipovaných technik modifikace povrchu byly vybrány dvě, které byly detailně zkoumány. Jedná se o depozici oxidu křemičitého (SiO_2) na povrch textilie, dále vystavení textilie působení ozónu spolu s depozicí SiO_2 a depozici oxidu titaničitého (TiO_2) na povrch textilie. Byly sledovány jednak mechanické vlastnosti upravené tkaniny, dále komfortní vlastnosti, odolnost proti bodání nožem a změny povrchu vláken.

Byla vyvinuta nová metoda pro aplikaci SiO_2 na povrch textilie s použitím vodního skla (WG) jako prekurzoru. Depozice SiO_2 byla analyzována a potvrzená pomocí skenovací elektronové mikroskopie (SEM), infračervené spektroskopie s Fourierovou transformací (FTIR) a spektroskopie rentgenového spektra (EDX). Koncentrace Byla nalezena významná souvislost mezi koncentrací WG a růstem QSKPR. Při koncentrací 40% WG ke zvýšení QSKPR o více než 200%. Navíc se ukázalo, že pro neupravené tkaniny vykazuje QSKPR specifický průběh pro různá KPA.

Depozice SiO_2 na tkaninu zvýšila koeficient tření vláken v tkanině. Ukázalo se, že u upraveného vzorku je třeba vyšší síly k rozestoupení přízí v tkanině než u vzorku neupraveného. Zvýšení koeficientu tření vláken ve tkanině s deponovaným SiO_2 bylo srovnatelné s tkaninou vystavenou působení ozónu s naneseným SiO_2. Nicméně u tkanin s naneseným SiO_2 byla zjištěna relativně vyšší ohybová tuhost.

Bylo zjištěno, že kvazi-statické pronikání nože je silně ovlivněno interakcí osnovních a útkových nití, což bylo popsáno modelem na bázi Fourierovy funkce. Tento model se dobře hodí pro hodnocení kvazi-statického pronikání nože pro různé tkaniny. Bylo také ověřeno, že kvazi-statické pronikání nože je přímo úměrné součiniteli tření tkaniny a nepřímo úměrné vzdálenosti mezi nitěmi.

Rozdíly v chování upravené a neupravené tkaniny při pronikání nože byly analyzovány pomocí CCD kamery během QSKPR měření. Bylo pozorováno, že klíčovou roli hraje profil nože. Tupá hrana nože zvyšuje odpor a na křivce tlakové síly způsobuje výrazný pík. Naopak po úplném proniknutí tupého kraje nože jsou jednotlivé nitě přeříznuty jedna za druhou. Lze konstatovat, že depozice částic SiO_2 zvyšuje tření mezi vlákny uvnitř příze, a proto se vlákna v upravené přízi chovají jako jednolitá masa proti ostré hraně nože.

Byl měřen odpor příze proti prokluzu, chování příze při řezání a síla nutná pro vytažení příze z tkaniny ve směru osnovy i útku v upravené a neupravené tkanině. Vyšší odolnost proti kvazi-statickému pronikání nože vykazuje osnova ve srovnání s útkem v obou textiliích (upravené i neupravené).

QSKPR byla měřena také na dvou vrstvách orientovaných vzájemně pod různým úhlem kladení (SA) tj. 0°, 45° a 90°. Bylo zjištěno, že SA 45° vykazuje relativně lepší odolnost proti kvazi-statickému pronikání nože do tkaniny. Stejné vrstvy případ byly vyhodnoceny pomocí testu podle modifikované normy NIJ-0115.00. Bylo zjištěno, že 45° SA vykazuje izotropní odolnost proti kvazi-statickému pronikání nože ve všech KPA. Upravené textilní struktury vykazují dvakrát vyšší odolnost proti kvazi-statickému pronikání nože než neupravené.

Klíčová slova: odpor proti prořezání; Oxid křemičitý; Oxid titaničitý; Ozón; Aramidy; vrstvené textilní struktury; vodní sklo

TABLE OF CONTENTS

1. Introduction

Protective textiles have become an important branch of technical textiles [1]. Textiles are playing a major role in wearables that assure life safety in various types of critical applications [2]. The introduction of gunpowder has changed the requirement of a body armour. The old solutions for body protection using metal and leather, silk or flak jacket armour became ineffective [3], [4]. Those solutions were no guarantee of life-saving against high-velocity gunfire or was bulky enough to restrict comfortable use [1]. The soft body light-weight armour became possible only after the birth of Kevlar® by DuPont™ in 1970s [5], [6].

In search of the best system of protection against ballistic threats, last few decades have produced considerable research on body protection armour. These armours are lighter than metallic armour solutions and easier to wear and carry. The solution was found in use of polymer-fibre composites, with synthetic fibres of high strength and high moduli like Dyneema®, Twaron®, and Kevlar® and thermoset polymer matrix. These solutions have better bulk properties and distribute the localized energy of impacting bullet to a larger area and dissipates its penetrating energy [7].

The latest requirement imposed on body protection armour is protection against sharp objects. Personal protection, against the attacks of sharp objects like the knife, has become increasingly important especially for police personnel [8]–[10]. The design of bullet resistant protection is different from the armour protecting against sharp objects like a knife or spike. In various condition of body protection against sharp objects and spikes is required. Such kind of attacks are evident where access to gunpowder and firearms is restricted by territory law, for example as in European countries or in prison facilities around the world [11], [12]. Generally, the bullet attacks are for army personals in some critical situation or in the battlefield, were the attack is expected. In contrast, sharp objects' attacks are unexpected, and the required period of protection is incessant and extended [13]. So, wearer's comfort also becomes a pre-requisite of armour design to produce light-weight and comfortable armour [14]–[17]. Also, the diversity of protection against various types of threats makes it difficult for a single solution to be viable in different kinds of situations. Generally, bullet resistant armour may not protect against knives or spikes or vice versa [18].

The characteristics of fibre-polymer composite inherit from the qualities of fibre and polymer to provide synergy for protection [19], [20]. In this scenario, it becomes important to study the response of stab resistance at the level of textile itself. This work is an effort in this direction and it investigates the interaction of knife and fabric.

2. Aims and Objectives

2.1. To study stab resistance of para-aramid woven fabrics at various knife penetration directions

Aramids are the one of the major class of fibres used in fiber-reinforced composites/laminates for soft and hard body protective systems [5]. And, it is proven that their longitudinal mechanical properties largely dominate their transverse characteristics. For example, compression, bending, and flexural properties are far weaker than tensile properties [21], [22]. The fibre damage results in delamination, cracking and fibrillation [23], [24]. However, it is preferably used in cut resistant and stab resistant application by commercial body protective products [25], [26]. The impact produced from symmetrical objects, like bullets in case of a

ballistic protection and sharp protruded objects like ice-pick in case of a stab resistance, is homogenous and generally perpendicular impact resistance is measured and reported and relative angle change between impacting object and resistance surface is not focused [15]. However, for the case of the stabbing of the knife the impact can be in various directions. It can be a fruitful study to observe how a para-Aramid respond when at least transverse angle of yarn with a knife is changed.

The most frequently followed methods of testing stab resistance performance are a drop-weight tower and quasi-static penetration of a sharp object into target textile protection [28]. In both these cases, the reported work, for textile fabric-based protection, a very small numbers of studies mentioned the measured angle of knife penetration [9] or tried to find out the effect of change in relative angle between attacking object and protecting surface [5, 16, 18]. However, the effect of blade orientation with respect to a single fibre and the single yarn was studied, which proved sensitivity of change in force required to cut the fibres or yarns with a change in cutting angle [30]–[34]. Cutting resistance is itself an intrinsic property of material but the orientation of fibrous assemblies in textile structure, their geometry and interaction of these elements within, can play a major role to improve cutting resistance. If we need to observe the cutting characteristics of textiles we need to see anisotropy at the material level (polymer and fibre level) and at textile structure level (yarn and fabric level). Since material level anisotropy is already highlight, there is a need to observe how woven fabric behave against change in orientation of knife stab.

2.2. To observe the interaction of knife and yarns of the fabrics

Out of the two methods of stab resistance measurements, the quasi-static method of loading provides the possibility of controlled perpendicular penetration. The provision of a pneumatic platform to hold the fabric in position, provides the ability to control the penetration at the specific orientation of knife blade with respect to the warp of the fabric. The results of stabbing are reproducible and provide the ability to record the interaction of knife and yarns of fabric on camera. While, the drop-weight tower is the accepted method of stab testing by NIJ, only measures if protection fails or not for given energy of penetration.

2.3. To observe the effect of change in friction on the stab resistance of fabrics

The force of friction is the major resistance against yarn movement and absorption of impact energy when no binding agent holds the yarns of fabric together. To change the friction between the surface of the yarn of woven fabrics were modified. But to keep the characteristics of soft body protection, the surface of fabrics was modified with minimal effect on their comfort properties, like air permeability and bending rigidity. The most economical ways of changing the surface for increased friction were adopted.

2.4. To observe the effect of stacking orientation and knife penetration direction

The orientation of different sheets in a stack, of multiple-layer laminate, can superimpose warp and weft of different sheets or can distribute them in different directions. It would be beneficial to observe if the super-imposing or distributing warp and weft of different sheets in multiple-sheets helps to improve stab resistance.

3. State of the Art

3.1. Structure and properties of para-Aramids

One of the most popular high-performance fibre used for the protective application is poly(para-phenylene terephthalamide) (PPTA), available with commercial names like Kevlar®

and Twaron® [7]. They are aromatic polyamides known as Aramids, that also includes *"a manufactured fiber in which the fiber forming substance is a long chain synthetic polyamide in which at least 85% of the amide (−CO−NH−) linkages are attached directly to two aromatic rings"* [5], [6]. Para-Aramids are high tenacity, high modulus fibres, they are gel spun from liquid crystalline solution, with a known structure as shown in Figure 1, and few of their mechanical properties are given in Table 1.

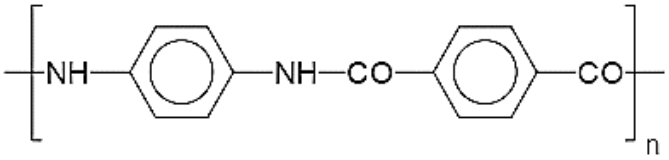

Figure 1: Polymeric Structure of Twaron® (poly-para-Phenylene-terephthalamide) (PPTA)

Para-Aramids were first produced for tire reinforcement [5], [6], [30] they are very anisotropic fibres in nature and split readily when mechanically fractured [30], [34]. They are highly crystalline and have long straight chain molecules aligned parallel to the fiber axis. In transverse direction to the fiber axis, they have Van der Wall's and hydrogen bonding which accounts for fibrillization and anisotropy of fibre mechanical character. These fibres show plastic deformation on compression that is the reason for their higher cutting strength and, therefore, is used in high impact protective textiles. [23]

Table 1: Para-Aramids Mechanical Properties [5]

Type of Fibber	Tenacity (*mN/tex*)	Initial modulus (*N/tex*)	Elongation at break (*%*)
Kevlar® 29	2030	49	3.6
Kevlar® 49	2080	78	2.4
Kevlar® 149	1680	115	1.3
Twaron®	2100	60	3.6
Twaron® High-Modulus	2100	75	2.5
Technora®	2200	50	4.4

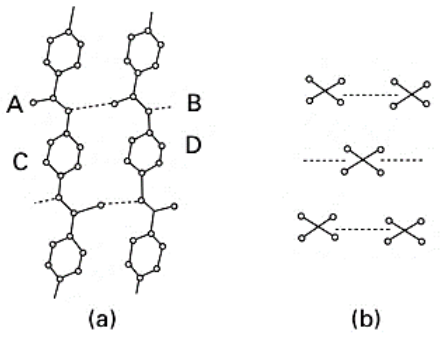

Figure 2: Showing molecular packing of PPTA crystal (a) hydrogen bonding in AB plane and absence in CD plane, (b) showing separate sheets when viewing along chains [23]

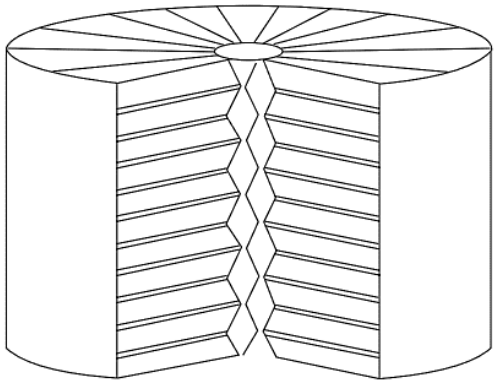

Figure 3: Radial pleated structure of para-Aramids [23]

The structure of PPTA crystal lattice is shown in Figure 2. It is observable that transverse plane, AB, having amide linkage, has a fewer density of covalent bonds than the plane, CD, having rings. Also, the amide linkage in the plane, AB, has a higher number of hydrogen bonding and, therefore, are firmer than the layer above and below to this plane (above and below the paper). That is the reason of anisotropy in a direction perpendicular to the fibre axis. Although fibre is highly crystalline and oriented at fine structure level, axial pleating of crystalline sheets exists in radial orientation as shown in Figure 3.

3.2. Role of Inter-yarn friction on impact loading

It has already been established that friction plays a very important role in resistance against impact loading [7], [35]–[37]. Increasing inter yarn friction can improve the performance against impacting load without added weight [36], [38]. A study has also highlighted the importance of yarn to knife and yarn to yarn friction during stab resistance [39]. The cutting force is dependent on the frictional coefficient and the normal force at the point of cutting during knife penetration [40]. There is another study about the cutting behaviour of knife/blade when it slides normally through the fabric. The outcome of the study reveals that there are two types of friction; macroscopic gripping friction and friction at the blade tip due to cutting of material. As the energy required to break the molecular chains is much smaller, most of the energy is dissipated in friction. Normal load produces friction at the edge of the blade. If the coefficient of friction between the blade tip and cutting point is increased the cutting resistance is reduced. But generally, the lateral gripping force is higher due to which the cutting resistance of the material is higher. Elastic modulus, the structure of material and velocity of the cutting blade significantly affect the friction and the resulting cutting resistance [31].

3.3. Anisotropic behaviour of High Modulus fibres against sharp blades

Mayo & Wetzel examined the failure stress of various organic and inorganic high performance single fibres when cut with the sharp blade, while cutting angle was changed from transverse to longitudinal orientation. They showed that the failure stress of both type of fibres was decreased by increasing the cutting angle while inorganic fibres exhibited less sensitivity to change in failure stress with the increase in longitudinal angle, Figure 4(a). It was also concluded that inorganic fibres fail in isotropic fracture while organic fibres, like para-aramids, had mixed mode of failure that involved cut failure, longitudinal and transverse tensile failure and transverse shear failure, owning to their structural anisotropy. [30], [33] Similar, studies on high performance Zylon® yarn [41] and Zylon®, Spectra® and Kevlar® yarns [32] concluded the similar results of the drastic decrease in yarn fracture energy as the knife cutting angle shifts from transverse direction to longitudinal direction, shown in Figure 4(b).

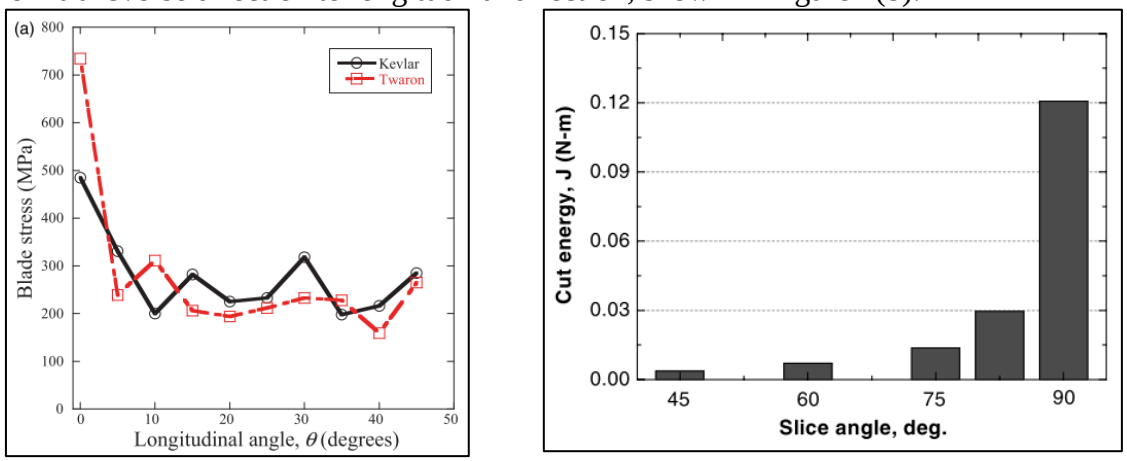

(a) (b)

Figure 4: (a) Cut resistance of single fiber para-Aramids measured at different cutting angles by Mayo & Wetzel [30], *(b) Effect of Yarn cutting angle on cutting energy measured by Shin & Shockey* [41]

3.4. Importance of Blade Orientation in Cutting Resistance of Fabric

Most of the research conducted to measure the stab resistance of woven fabrics does not mention the knife penetration angle. Either fabric is loaded without mentioning the knife penetration angle [42], [43] or one angle is selected [9] and comparison of different angle is not made. However, very few studies mentioned the effect of change in knife orientation with respect to protective fabric.[27], [29] These studies showed that changing relative angle between knife penetration direction and surface of textile significantly affect the resistance of protective textile [44]. However, such study that involves observing the knife's transverse orientation with respect of warp and weft of fabric is not yet performed. This suggests investigating if such anisotropic behaviour of stab resistant in such orientation of knife and fabric is present.

3.5. Effect of plies orientation textile resisting against impacting load

Importance of orientation of plies in resisting against ballistic impact situation is already established. The literature established this fact either numerically [45], [46] or/and experimentally. It has been shown that plies oriented at an angle can absorb up to 20% higher amount of impact energy than aligned plies. There is an optimum level of plies orientation that improves this impact resistance [46]. However, the effect of orientation of plies on stab resistance could be a good area of study. It can verify the benefits of angle plied achieved in ballistic impact for knife stabbing resistance.

4. Materials and Methods:

4.1. Materials:

4.1.1. Fabric

Woven fabric investigated in this research was composed of high modulus multifilament Twaron® 2200 yarns, with linear density of 1620 *dtex* (1000 filaments, 5.86 *TPM*). The weave of the fabric was 1/1 plain and a balanced construction, with equal yarn linear density and equal set of warp and weft was used. The style of the fabric was KK220P and it was sourced in loom state from G. Angeloni srl Italy. The greige fabric was having an areal density of 220 g/m^2. [47]

Table 2: Fabric Parameters

ID	Warp / Weft Yarn	Weave	Warp Sett (*ends/cm*)	Weft Sett (*picks/cm*)	Areal Density (g/m^2)	Thickness (*mm*)
Off-Loom	Twaron ® 2200 (1000 f) 1620 *dtex*	1/1 Plain	6.45	6.34	220	0.28
Neat			6.41	6.40	218	0.32

The detailed specifications of Neat fabric are given in Table 2. The optical micrographs of treated and untreated fabrics are shown in Figure 5.

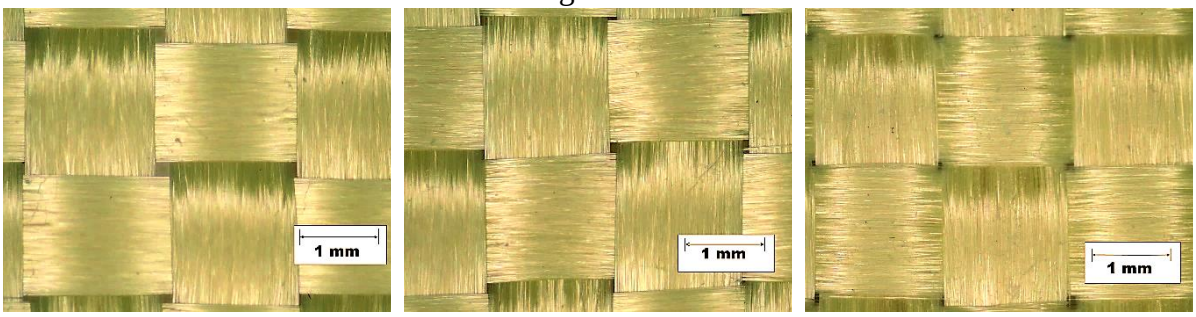

(a) (b) (c)

Figure 5: Microscopic image of (a) Neat, (b) S3 and (c) S4 fabrics

4.1.2. Water Glass

Sodium Silicate aqueous solution (36-40% concentration) is a low-cost product, available in market, known as Water Glass, is used as source of SiO_2. It contains Sodium Oxide (Na_{2Z}) and Silicon dioxide (Silica, SiO_2). It is an industrial product and is used in various industries like detergent, paper pulp bleaching, municipal and waste water treatment, concrete, abrasive and adhesive [48].

The water glass (VODNÍ SKLO Vízuveg of KITTFORT, CAS: 1344-09-8) is used as a precursor of SiO_2 in the current study. It has been reported to be a silica source [49]. It is alkaline in nature and precipitates into SiO_2 when reacted with weak acid, like acetic acid. A generalize reaction of SiO_2 deposition can be given as:

$$Na_xSi_yO_z \xrightarrow{H^+} SiO_2 + Na^+ \quad (1)$$

4.1.3. Titanium dioxide (TiO_2)

Titanium dioxide used in this work is (AEROXID® TiO_2 P25 by EVONIK INDUSTRIES) a hydrophilic fumed powder. It has high purity ($TiO_2 \geq 99.50\%$) and high specific surface area of 35-65 m^2/g. It consists of primary aggregate of partials with an approximate partial size approximate 21 nm and density 4 g/cm^3. Anatase to Rutile weight ratio of 80/20 [50], [51].

4.2. Methods

The summery of methods followed in this work is shown as tree diagram in Figure 6.

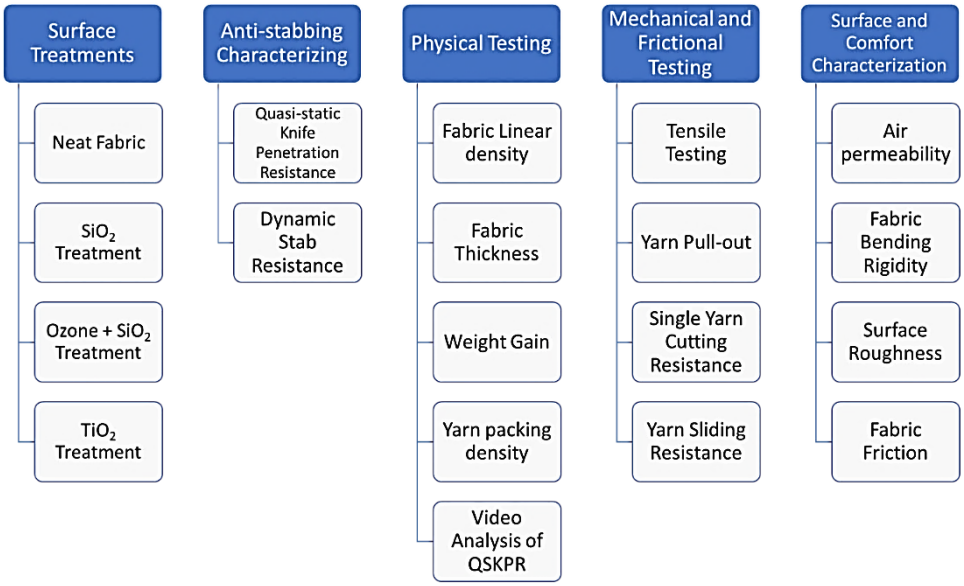

Figure 6: Summery of methods followed in this work

4.2.1. Surface Modifications

4.2.1.1. Neat Samples Preparation

Before any chemical application the surface of raw samples was made clear from process add-ons that may have been applied on the fabric surface. For this purpose, different trials were made and finally Methanol washing was chosen as sufficiently effective method. So, 99.99% Methanol, (CH_3OH) (P-Lab Czech Republic), washing was conducted for 3 *min* in a vibrating bath (at 150 *rpm*), with a bath ratio 1:50. Afterwards, samples were rinsed and dried. The fabric samples in this state are called "Neat" samples and used as "untreated" fabric for comparison with surface modified samples. Neat samples are denoted with "N" in this work. The process of methanol washing is illustrated in Figure 7(a).

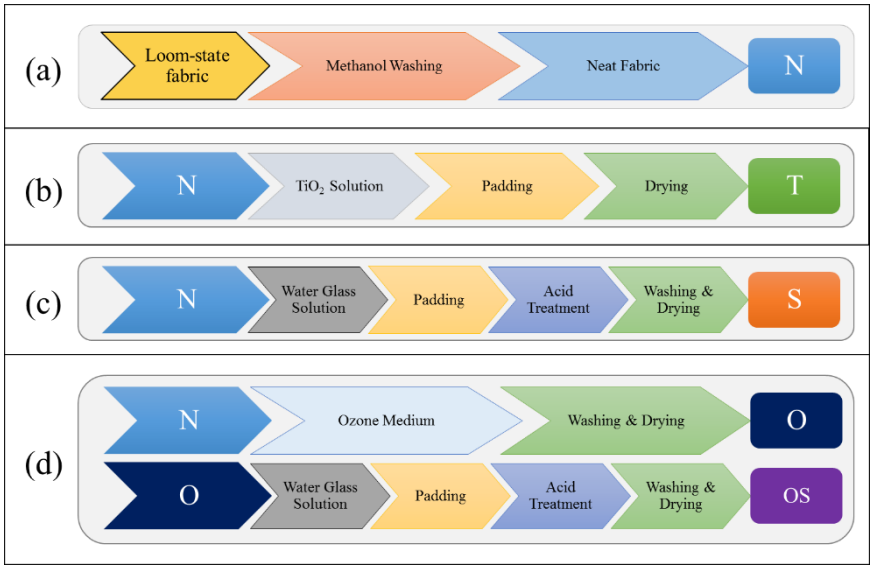

Figure 7: Step of surface modifications for different techniques, (a) Methanol Washing steps for Neat samples, (b) Steps followed for TiO_2 Treatment, (c) Steps followed for SiO_2 treatment, and (d) Steps followed for Ozonization and post-treatment with WG

4.2.1.2. Surface Modification by SiO_2

WG, used in this work, was 40% aqueous solution of Sodium Silicate. It was diluted to different concentrations to produce S1, S2, S3 and S4 samples, details can be found in Table 3. Each of these sample was immersed in Sodium silicate solution. And was padded at squeezing pressure of 1 *bar* at linear speed of 1 *m/min*, to gain a wet pick up of 50±10%. The samples were then immersed in 5 *g/l* Acetic acid for 15 *min*, a bath ratio of 1:20 was maintained enough to dip the samples well in the solution. To facilitate the reaction and deposition of SiO_2 the container was continuously shaken at 150 *rpm*. After that it was rinsed and hot-air oven dried. An illustration can be found in Figure 7(c).

Table 3: Different concentrations of Sodium silicate solution

Sample Identification	S1	S2	S3	S4
Water Glass Conc.	4%	8%	20%	40%

4.2.1.3. Surface Modification by Titanium dioxide

Aqueous solution of hydrophilic TiO_2 was prepared with the help of sonification. The concentration of TiO_2 was increased from 0.01 *g/l* to 0.5 *g/l* in five different solutions as identified in Table 4. Each sample was dipped in respective solution of TiO_2 with a liquor ration of 1:25. Roller padding was followed with nipping pressure of 1 *bar*, followed by hot-air oven drying at 100°*C* for 10 *min*, the process is illustrated in Figure 7(b).

Table 4 Details of different TiO_2 Solutions

Sample Identification	T1	T2	T3	T4	T5
TiO_2 Concentration (g/l)	0.01	0.05	0.1	0.25	0.5

4.2.1.4. Ozone Application

Ozone medium was prepared from distilled water in which weighted fabric samples were immersed. The oxygen was concentrated by Kröber O2 (Kröber Medizintechnik GmbH, Germany) at 3.0 *l/min* flow rate. The Ozone gas was generated by Ozone Generator TRIOTECH GO 5LAB-K (Czech Republic), and its concentration was monitored by

LONGLIFE TECHNOLOGY LF-2000. At the end of the stream flow Ozone gas was destroyed. The set-up of application of the Ozone medium is illustrated in Figure: 8.

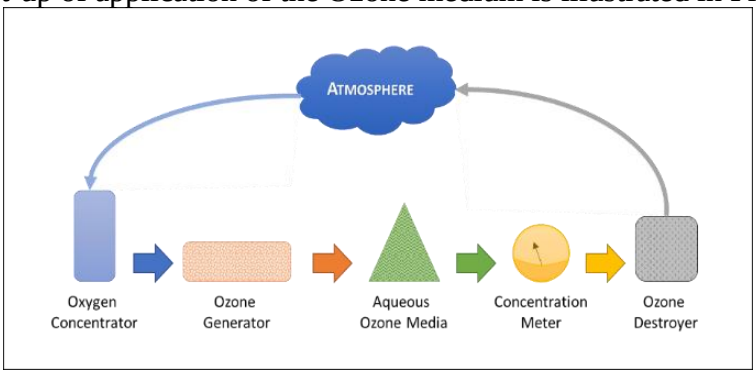

Figure: 8 Illustration of Ozone Medium Set-up

Neat fabric samples were exposed to the Ozone in the aqueous medium, for 60 and 120 *min*. To check the combined effect of Ozone and WG, 120 *min* ozone treated samples were, also, deposited with SiO_2 (*following the same procedure as described in 4.2.1.2 for Neat samples*). The details of exposure time of these samples are given in Table 5 and treatment steps are shown in Figure 7(d).

Table 5: Details of Ozonized and SiO_2 Deposited Samples

Sample Identification	1Z	2Z	2ZS3	2ZS4
Ozone Medium Exposure (*min*)	60	120	120	120
Water Glass Concentration	-	-	20%	40%

4.2.2. Stab Resistance Measurements

4.2.2.1. Details of Knife and Measurement Procedure of Quasi-Static Knife Penetration Resistance (QSKPR)

The testing procedure, for the measurement of quasi-static knife penetration resistance, was in accordance to recently reported method followed by various researchers. [28], [40], [52], [53].

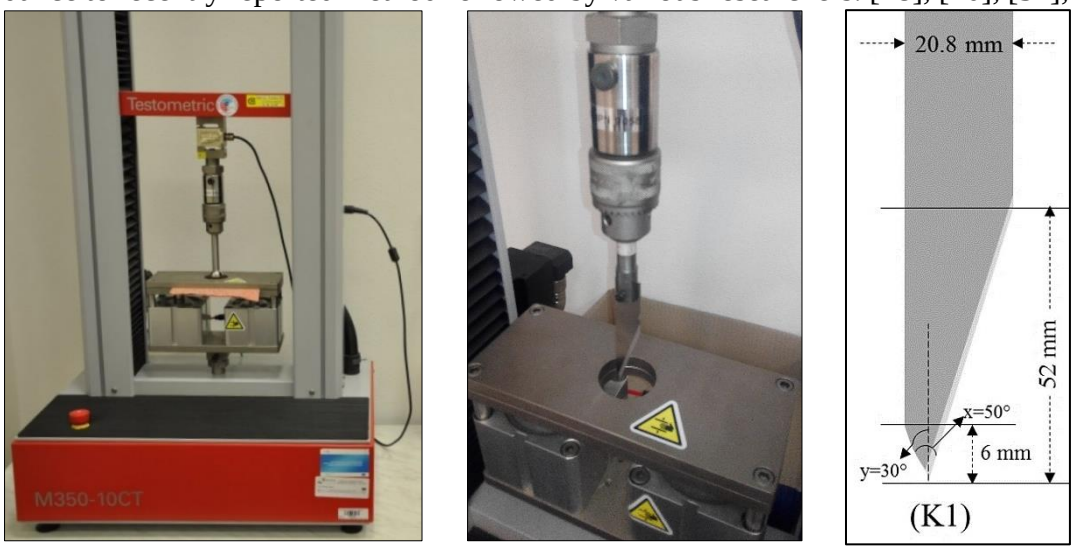

(a) (b) (c)

Figure 9: (a) Universal Testing Machine (TESTOMETIC M350-10CT), (b) Cross-head installed with knife and (c) Geometry of CKB-2 (K1)

Universal testing machine TESTOMETIC M350-10CT, shown in Figure 9(a), was used to penetrate the fabric samples quasi-statically at constant rate of penetration of 8.33 mm/s. The fabric held in a pneumatically operated platform at 7.5 *bar* with inner diameter of circular opening of 45.55 *mm*. Samples were pre-tensioned at 1 *N* force. Samples size of each fabric

sample was 100 *mm* x 100 *mm* ±5 *mm*. The knife was held in cross-head with 1000 *N* load cell and was vertically penetrated the fabric for 42 *mm*. Its response in terms of force-displacement curve was recorded and force at peak resistance was noted.
The knife material, shape and sharpness directly effects the response of the fabric. [11], [32], [41], [44], [54] Owing to this important factor the knife used in this procedure, was wood crafting stainless steel knife, namely CKB-2 of OLFA Japan. To obtain consistent shape and sharpness for different measurements, commercially available knives were utilised.
The shape of knife can be observed, as K1, in Figure 9(c). It is visible that one edge of knife is sharp and other side is blunt. The first 6 *mm* of the tip of knife profile has inclination on both direction with 50° angles while after this tip the blunt side is parallel to the length of knife. While sharp edge has 15° inclination for a maximum vertical length of 52 *mm*. Maximum width of knife is 20.8 *mm* and thickness of 1.2 *mm*. One important observation must be noted here that width of the knife (that causes cut in the fabric) increases rapidly for first 6 *mm* due to both-sided inclinations, however, after that knife profile width increases in single-side corresponding to 20° angle of inclination. To keep the knife to knife sharpness variation, on average, one knife was used for a set of 18-24 samples, with equal probability of selection among different KPAs.

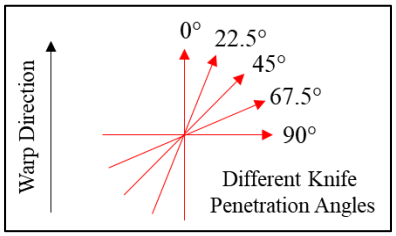

Figure 10: Illustration of different Knife Penetration Angles

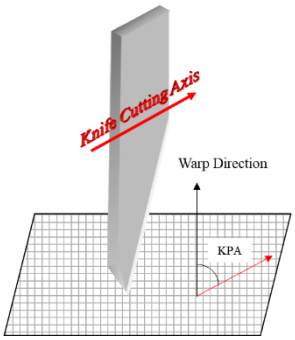

Figure 11: Illustration of knife cutting axis

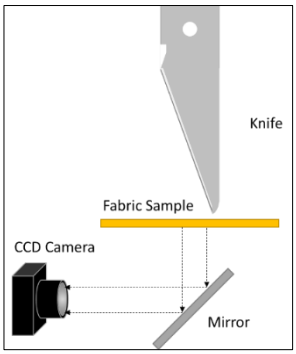

Figure 12: Camera Set-up for tracking knife penetration

The QSKPR was tested for five different Knife Penetration Angles (KPA= α = 0°, 22.5°, 45°, 67.5°, and 90°), as illustrated in Figure 10. KPA here refers to the angle made between axis of warp yarn length and blade cutting axis, while blade penetrates the fabric vertically downwards, as illustrated in Figure 11. For each KPA at least 10 samples were tested for single sheet stack and 6 samples for multiple sheet stack, and mean results were computed.

4.2.2.2. Video Analysis Setup

The interaction of knife and fabric samples during QSKPR measurement was recorded on video using SONY HDR-SR12E camera at 25.0 *fps*. A setup was developed to reflect rare side of fabric penetration to focus at camera lens, as shown in Figure 12.
Each frame of recorded video was separated into an image file using MATLAB program. The extracted frames were analysed to observe the interaction of knife with each yarn fractured. By using image analysis software, Digimizer, knife edge displacement and strain of each yarn was measured before rupture. Then comparison of Neat and S4 fabrics was conducted, found in section 5.6.

4.2.2.3. Dynamic Stab Resistance (DSR) Measurement Procedure:

DSR was performed following the modified version of NIJ Standard–0115.00 [55]. The drop-weight tower testing equipment was used, as shown in Figure 13(a), and damping material layers shown in Figure 13(b). K1 knife was used to penetrate for DSR, consistent with QSKPR

measurements. The effect of change in knife penetration angle on stabbing resistance was observed, while density of the samples was kept similar. Change in penetration depth for two potential energies, of dropping knives 0.74 *J* and 1.47 *J*, was compared.

Table 6: Dynamic stab resistance Samples details (95% confidence interval in parenthesis)

Fabric ID	Sheets	Stacking Angle	Areal Mass (g/m^2)	Thickness (mm)	Fabric Density ρ [kg/m^3]
N	8	45°	1765	2.60 (±0.02)	678.85
S4	8	45°	1812	2.73 (±0.04)	663.74

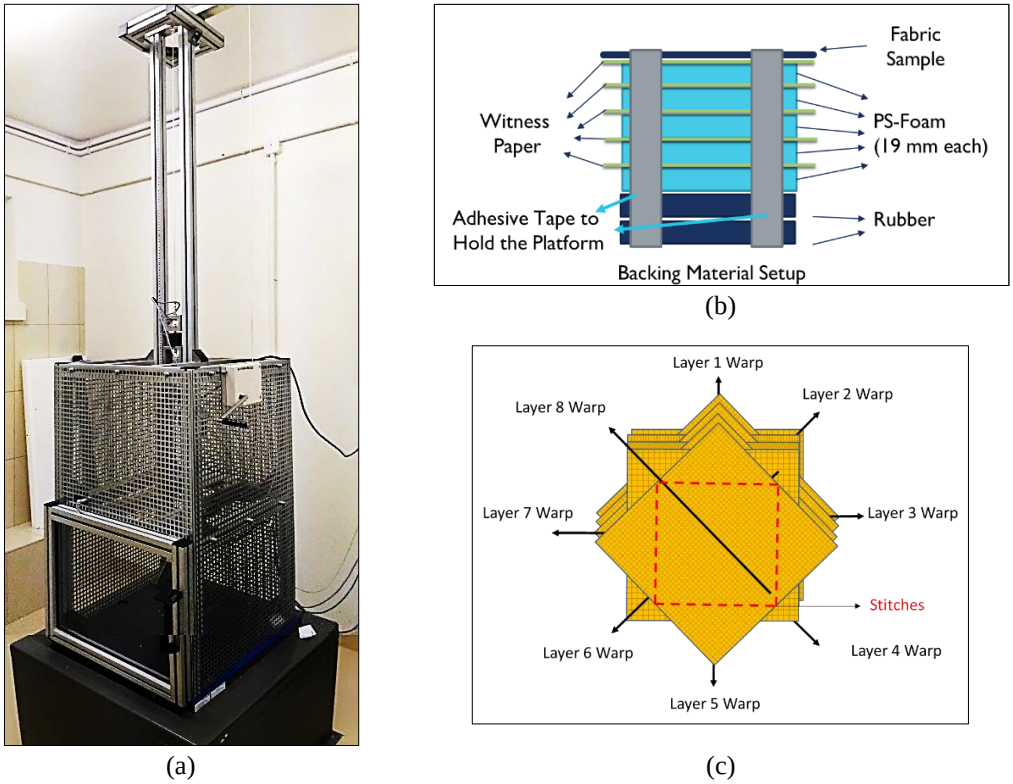

(a) (b) (c)

Figure 13: (a) Drop-weight measurement set-up for DSR, (b) Backing / Damping material arrangement and (c) Illustration of 8 sheets stacking orientation

The drop-weight measurement equipment was available with laser distance measurement device with high accuracy. The knife was dropped under gravity from two fixed heights of 10 *cm* and 20 *cm*. The data was recorded by a custom written program in National Instrument Software that acquires the data from load cell, distance measurement sensor and accelerometer and presents data for acceleration, drop distance, resistance force with sampling rate of 50 μs. DSR of different samples were compared for KPA of 0°, 45° and 90°. Eight sheets of single layer fabric sample were placed one over another at 45° stacking angle and were sewed, illustrated in Figure 13(c). The details are available in Table 6.

4.2.3. Imaging and Topography Analysis

4.2.3.1. Fourier Transformation Infra-Red (FTIR) spectroscopy

To verify the chemistry of the deposited layer, the treated samples were analysed for Fourier Transform Infra-Red (FTIR) spectroscopy. A Thermo Fisher FTIR spectrometer, model Nicolet iN10, was used in this work.

4.2.3.2. Scanning Electron Microscopy (SEM)

Fabric samples were also scanned for their surface topological differences using Scanning Electron Microscope (SEM) VEGA TESCAN TS5130 at 20 *KV* for 2000X magnification. Fibres removed from post-penetrated fabric samples in quasi-static knife penetration resistance testing were also scanned to observe the plastic deformation mode.

4.2.3.3. Energy-Dispersive X-ray (EDX) Spectroscopy

To observe the atomic composition of deposited layer, EDX was performed at 20 *KV*. The atomic composition of treated and untreated surfaces was determined. The peaks of the detected elements were obtained, and percentage composition was computed.

4.2.3.4. Optical Microscopy

Optical microscopy was conducted to observe the surface changes and structural parameters. For the structural measurement image analysis was performed. To obtain the fabric cross-sectional images, fabric samples were immersed in epoxy resin, cured, dissected and polished. Afterwards, microscopic images were taken under different lighting conditions.

4.2.3.5. Laser Scanning Confocal Microscopy (LSCM)

To observe the microscopic changes at knife cutting edge, it was 3D scan using LSCM. Laser scanning helped generates three-dimensional surface map. Scanned data was analysed for roughness at tip of knife edge and change in its sharpness after stabbing.

4.2.4. Mechanical Characterization

4.2.4.1. Tensile Testing

The tensile strength of warp and weft yarns removed from different fabric samples was recorded. Measurements were made following the ASTM D2256 standard; on Universal Testing Machine TIRATEST. Samples gauge length was 20 *cm* with loading speed of 100 *mm/min*. 20 samples were tested for each selected set of yarns.

4.2.4.2. Yarn Pull Out

To observe the interaction of individual yarn with interlacing yarns yarn pull out test was carried out. The method followed is in accordance with already available in literature [56]. The details are described as follows:

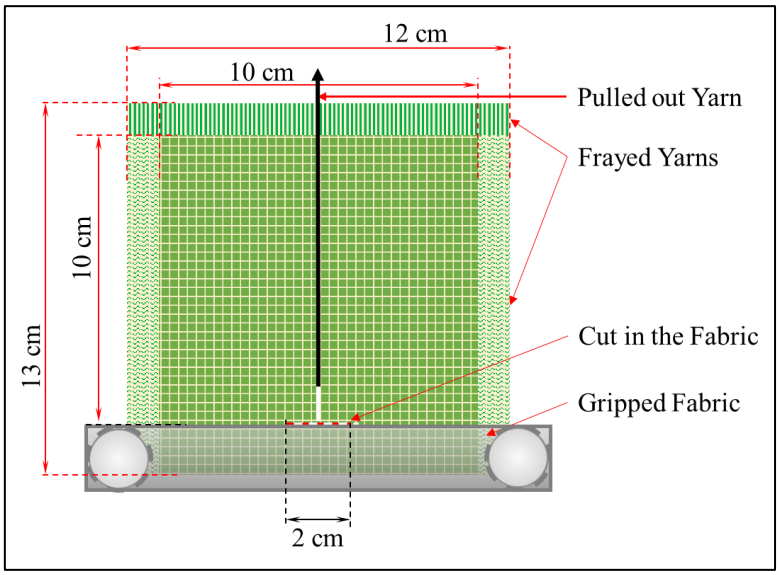

Figure 14: Description of yarn pull-out setup

A rectangular sample of size 12 × 13 cm^2 was taken. Fabric was unravelled 1 *cm* from three sides, skipping the side that is to be gripped, as shown in Figure 14. A cut of 2 *cm* was made, as shown by red dashed line, at distance of 2 *cm* from edge, to make the pulling yarn's one end free. The cut was made exactly at the centre, which makes sliding end of pulling yarn free. The pulling yarn was gripped in tensile machine's jaw from frayed side of sample. Force-displacement curve was plotted for complete pull-out of yarn. At least 10 samples for each fabric direction, warp and weft, was measured. The average resistance offered by each interlacement was also computed.

4.2.4.3. Individual Yarn Cutting Resistance

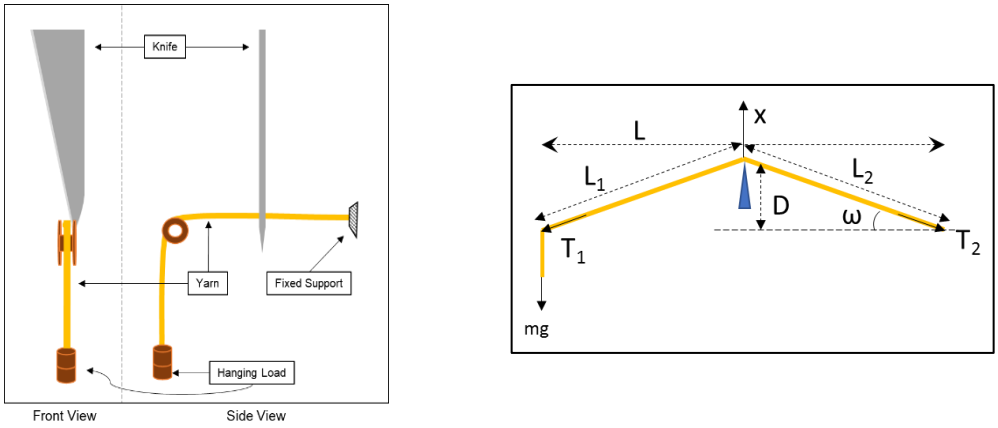

(a) (b)

Figure 15: (a) Illustration describing setup for individual yarn cutting resistance measurement and (b) Free body diagram for resolution of forces at yarn rapture point

To find out cutting resistance of single yarn, warp and weft yarns were removed from Neat and S4 fabrics. A custom-made yarn holder was used to present the yarn to universal testing machine. One end of each yarn was tied with the fixed support and other was hanged through a free pully with a constant load. The yarn with minimum constant tension, 2.18 *N*, was introduced in front of the sharp edge of knife. The knife contacts the yarn at midpoint of length L and divides it into two components L_1 and L_2. The knife was fitted to cross-head of the universal testing machine through a 50 *N* load cell that was operated at 8.33 *mm/s* vertically downwards while knife edge displaces the yarn horizontally in x direction as represented in Figure 15(b). The force and vertical displacement were noted for each individual yarn for its complete cutting, and energy was computed. As knife sharp edge make constant angle with its vertical length the corresponding knife edge travel D was computed and reported. The setup is shown in Figure 15(a) and free-body diagram in Figure 15(b). The details of testing results can be found in section 5.7. The objective was to observe the force and energy required to cut individual yarns, at minimum constant yarn tension.

4.2.4.4. Yarn Sliding Resistance

The penetration of knife into the fabric cause formation of a slit that is made by cutting the yarns coming in way of the knife edge. If there is no fracturing of the yarns by knife, the knife penetration would only displace the yarns. It is the sharp edge of the knife that cut through the yarns before displacing the yarn to a considerable distance. Through video analysis it was observed that extent of each yarn sliding before cutting by knife is between 1 to 2 *mm* (Figure 37(b)) before it is fractured. So, an experiment was designed to see the resistance offered by different fabrics when yarns in the fabric are displaced without fracturing.

In this devised method, a very fine (0.1 *mm*) thickness steel wire was used to hold the lower part of the fabric while a loop, of the same wire, was passed through the fabric to be fixed in

the upper jaw of universal testing machine. The bottom 1 *cm* of fabric sample was fixed in lower jaw along with the fixed wire. The sample size was 10 × 11 *cm*. The setup devised is illustrated in Figure 16. Each fabric sample was displaced to maximum 10 *mm* distance and force-displacement response was recorded. The cross-head was operated at constant speed of 100 *mm/min*, with a load cell of 100 *N*. The results of yarn sliding resistance can be found in section 4.2.4.4.

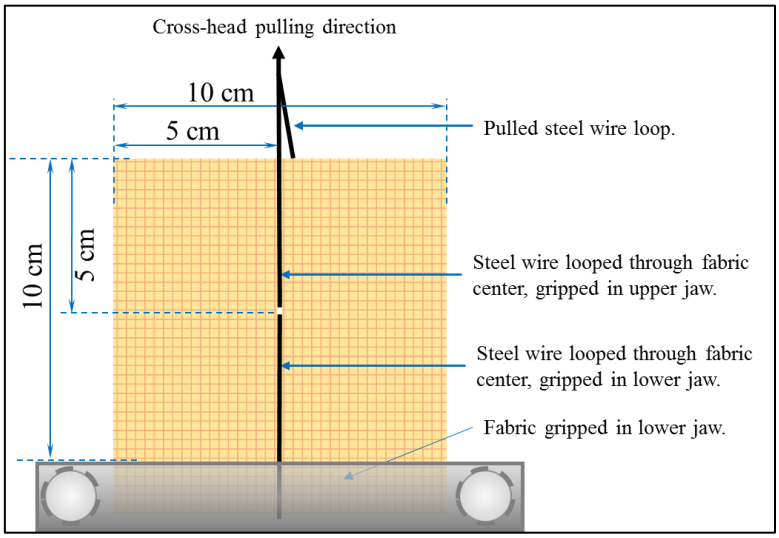

Figure 16: Yarn sliding resistance measuring setup

4.2.5. Comfort and Friction Characterisation

4.2.5.1. Air Permeability

Air permeability of different samples were measured using air permeability tester (FX-3300) following the standard method ISO9237.

4.2.5.2. Surface Feel and Comfort Properties

Effect on comfort and fabric touch characteristics was analysed using M293 Fabric Touch Tester of SDL Atlas. Fabric bending rigidity, thickness, surface friction, and surface roughness were measured. Measurements was made at face and back of the samples and average was recorded.

5. Results and Discussions:

All the results mentioned in this work represents the mean values of the corresponding measurements. The error bars in figures and values in parenthesis represent the 95 % confidence interval (CI), unless specifically mentioned otherwise.

5.1. Comfort Characterization:

5.1.1. Air permeability

Air permeability of various fabrics was measured using the procedure mentioned in section 4.2.5.1. The results are shown in Figure 17. The higher air flow through ozone treated samples in comparison to Neat fabric indicates that Ozone application makes structure more open. While air permeability of SiO_2 deposited fabric reduces significantly. Therefore, it can be inferred that increasing amount of deposited SiO_2 fills the fabric pours and fabric become less permeable to air.

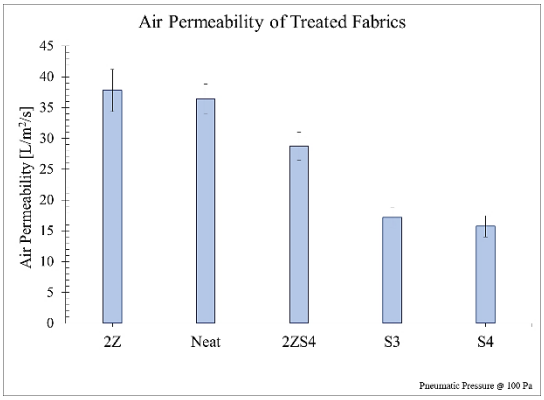

Figure 17: Air permeability of various treated fabrics

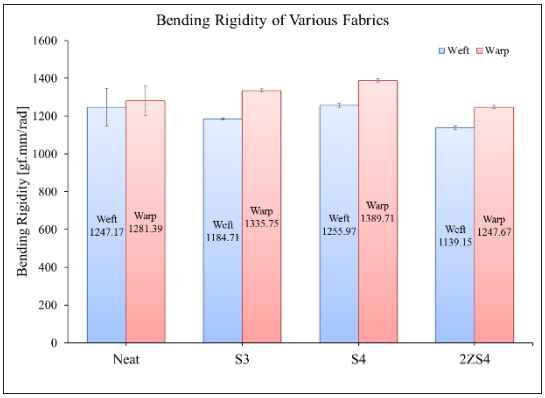

Figure 18: Bending rigidity of treated and untreated fabrics

5.1.2. Bending Rigidity

The bending rigidity was measured using Fabric Touch Tester. The bending rigidity of various fabrics were measured at face and back of each fabric, in warp and weft directions, and their mean was computed. Bending rigidity, along warp and weft, of various fabrics is shown in Figure 18. It is apparent that SiO_2 treatment turned fabrics more rigid, while ozonized fabric, even after treatment with SiO_2, is found to be most flexible of all treated and untreated fabrics.

5.1.3. Coefficient of Friction

The coefficient to friction of various fabrics were measured using Fabric Feel Tester the average measured values in warp and weft direction can be found in Figure 19. It is evident that the application of SiO_2 has increased the coefficient of friction. The order of increase in friction from least to highest friction is like: Neat → S3 → 2ZS4 → S4.

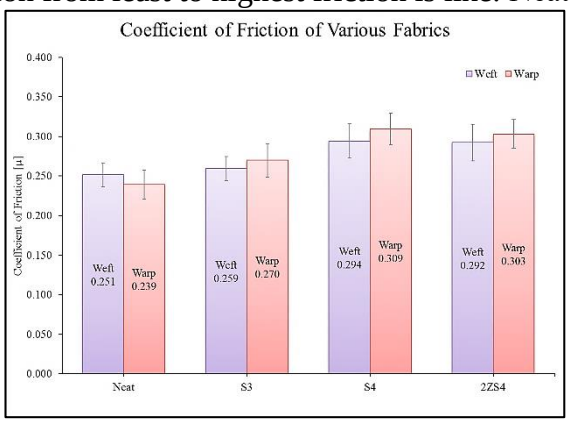

Figure 19: Change in coefficient of friction from Neat to treated fabrics

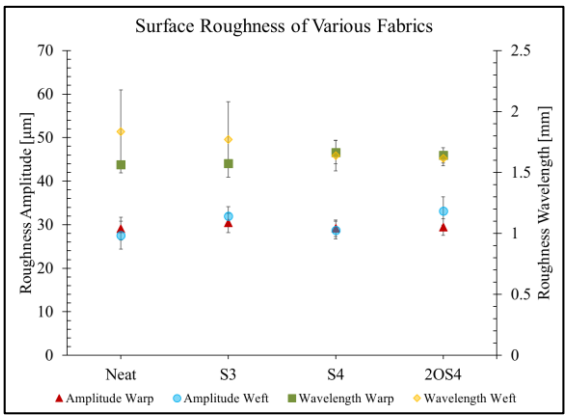

Figure 20: Surface roughness in terms of waviness amplitude and wavelength

5.1.4. Surface Roughness

The surface roughness was measured using Fabric Feel Tester, the results are shown in Figure 20. From these results it can safely be said that there is not much change in roughness of the fabric samples before and after treatment, however, weft of Neat and S3 shows some variability in the wavelength of waviness.

5.2. Effect of Different surface modifications on QSKPR and Penetration Energy

5.2.1. Silicon dioxide Deposition

Neat fabric was treated with WG in four different concentration (4%, 8%, 20% and 40%) using padding rollers followed by acid treatment to deposit SiO_2 layer as described in section 4.2.1.2.

Each fabric was tested for QSKPR in three different KPA (0°, 45° and 90°) and their mean QSKPR and penetration energy at peak resistance was computed.
It was founded that, on increasing the concentration of WG directly proportional increase was observed in QSKPR and penetration energy (PE) at peak resistance, as shown in Figure 21. The coefficient of the first order polynomial model fitted to the data, along with goodness of fit, can be found in Table 7.

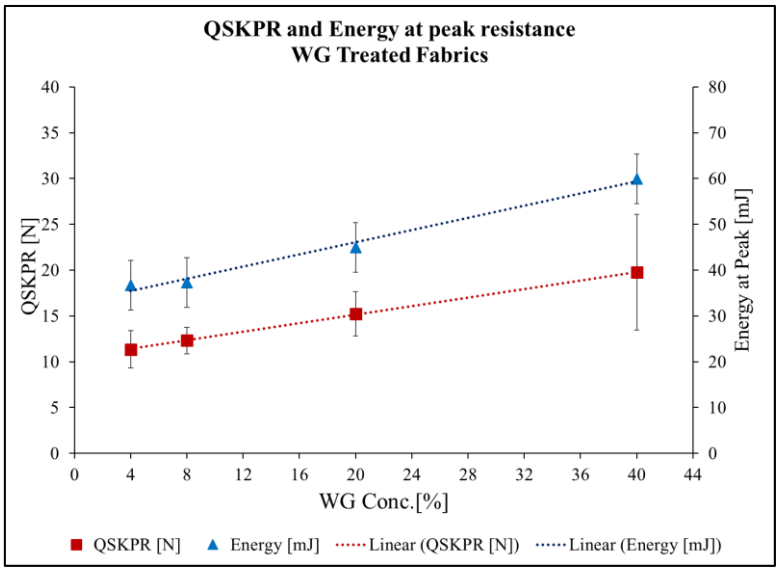

Figure 21: Effect of WG treatment on QSKPR and Energy at peak resistance

Table 7: Coefficients of 1st degree polynomial fit for QSKPR and PE vs WG Conc. and goodness of fit

Coefficients of Model (*Upper and lower bound of 95% CI*)	p_1		p_2	
QSKPR	0.233 (0.221, 0.246)		10.47 (10.19, 10.75)	
PE	0.666 (0.456, 0.876)		32.75 (27.95, 37.54)	
Goodness of fit	**SSE**	**R-square**	**Adjusted R-sq.**	**RMSE**
QSKPR	0.0131	0.9997	0.9995	0.0810
PE	3.745	0.9893	0.984	1.368

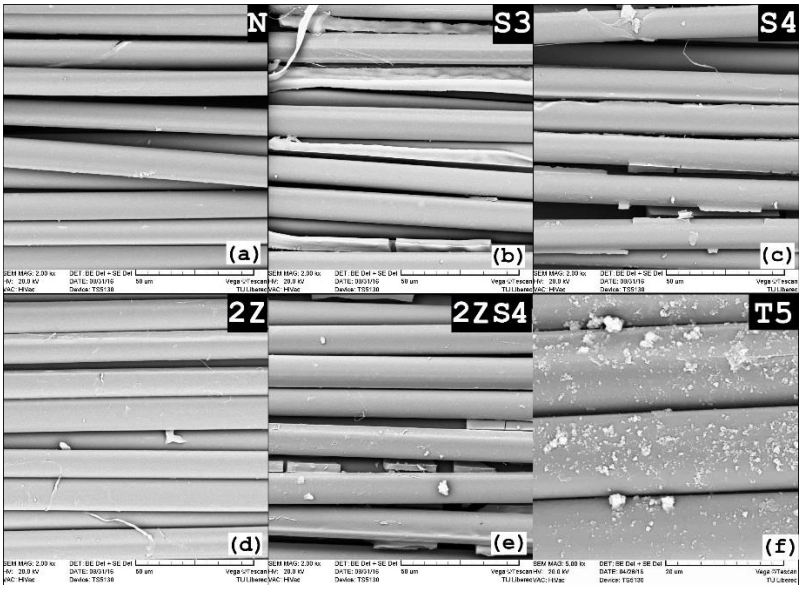

Figure 22: SEM images of different treated samples showing surface topography of (a) Neat, (b) S3, (c) S4, (d) 2-hour Ozone treated, (e) Ozone and WG treated and (f) Titanium dioxide treated T5 fabric samples

It is judged that on increasing the concentration of WG results higher amount of SiO_2 deposition, as is evident from weight gain of up to 8% for S4, the deposited layer is observable in SEM images in Figure 22(b) & (c). The deposition of SiO_2 makes yarn stiffer and increase the fabric's coefficient of surface friction. Also, the air permeability results showed the pours are filled with deposited layer which reduced the air permeability significantly for SiO_2 deposited fabrics. Also, fabric density (mass per unit volume) increased due to the higher compactness of the fabric. All these parameters are adding to increase the QSKPR and PE at peak resistance.

5.2.2. Ozone and WG Treatment

It is believed that Ozone treatment can affect the para-Aramid [57]. Therefore, Neat samples were exposed to aqueous ozone medium for 60 and 120 minutes. The Ozone treatment setup and procedure is described in section 14.2.1.4. The results of these treatments as comparison of fabric treated with Ozone only and with Ozone and WG is shown in Figure 23 and effect of WG concentration on 2ZS4 fabric is shown in Figure 24 and their coefficient of first order polynomial fit and goodness of fit in Table 8.

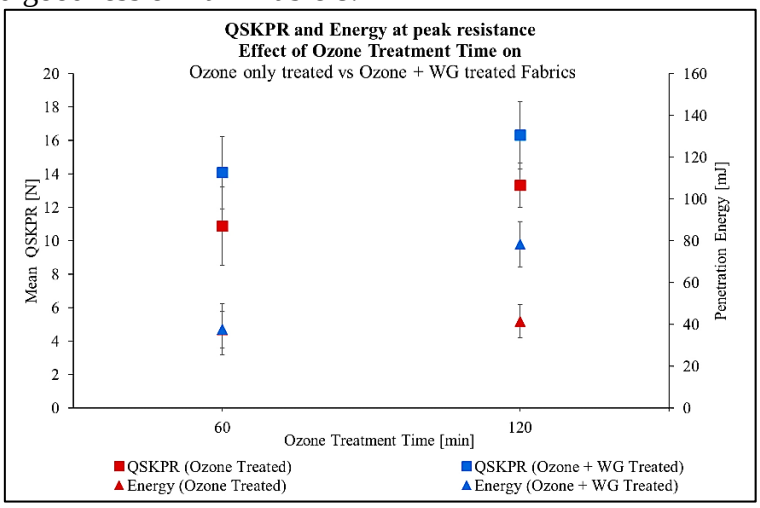

Figure 23: Effect of Ozone treatment time on Ozonized only and Ozone + WG treated fabrics

Table 8: Coefficients of 1st degree polynomial fit, for QSKPR and PE vs WG Conc. and goodness of fit, for 120 min O_3 Treatment

Coefficients of Model (***Upper and lower bound of 95% CI***)	p_1		p_2	
QSKPR	0.2489 (-0.4823, 0.9802)		12.68 (-6.205, 31.56)	
PE	2.139 (-0.05399, 4.333)		39.55 (-17.08, 96.18)	
Goodness of fit	**SSE**	**R-square**	**Adjusted R-sq.**	**RMSE**
QSKPR	2.65	0.9493	0.8985	1.628
PE	23.84	0.9935	0.9871	4.882

Ozone treated samples did not showed any physical changes at the fibre surface, as is observable in SEM images shown in Figure 22(d), unchanged flat surface is resembling the Neat fibres as seen in Figure 22(a). The ozone treatment improved the comfort and mechanical properties, as discussed in section 5.1.2, but its stab resistance performance was not significantly improved, as shown in Figure 23. However, ozonized samples were also treated with WG and fabric with both treatments showed proportional increase in QSKPR and penetration energy as WG concentration was increased, as shown in Figure 24. Although, only WG treated fabrics had better QSKPR but ozonized and SiO_2 deposited samples had comparable QSKPR, as found in Figure 27, with better comfort properties. It can be observed

that 2ZS4 has comparatively less air permeability and lesser bending rigidity, as shown in Figure 17 and Figure 18 respectively.

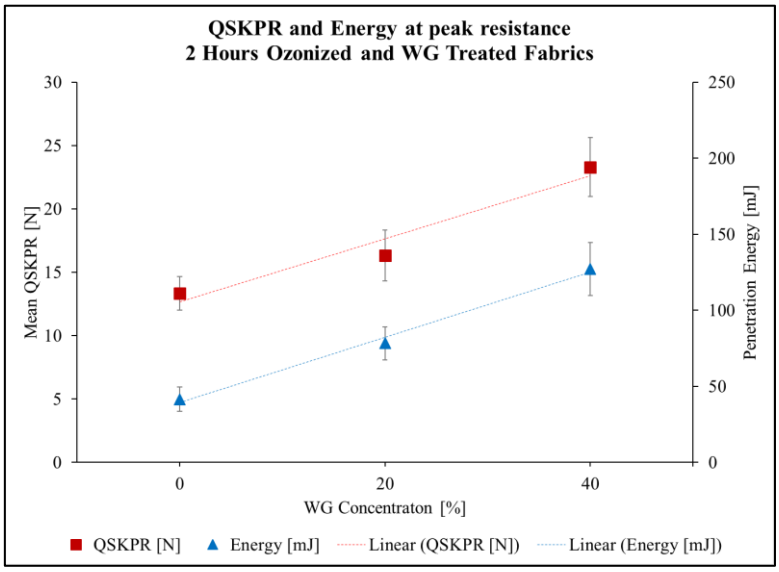

Figure 24: Effect WG concentration on QSKPR and Penetration Energy of Ozonized and WG treated fabrics

5.3. Deposition of the SiO_2 Layer

The deposition of SiO_2 layer was verified by following surface analysis techniques.

5.3.1. SEM images:

The physical presence of the deposited layer was observed in SEM images as shown in Figure 22(a), (b) and (c), for Neat, S3 and S4. Fabric surface topologies, of these fabrics, are confirming the physical presence of the deposited layer. For S3 and S4 samples, the deposited layer is apparent not only on the fibres surface but also in the gaps between fibres. Additionally, S4 sample shows the irregular edges of the deposited layer. In contrast, the untreated Neat sample has the smooth and clear surface.

5.3.2. FTIR Spectroscopy

The FTIR spectra of treated and untreated samples are shown in Figure 25. The peak between 1000 to 1100 cm^{-1}, for silica powder curve, is due to the characteristic stretch vibration of Si-O [58]. The differences, in the curves of the untreated and the treated samples indicate the changes occurred after SiO_2 layer deposition. This change is noticeable in curve of treated fabric where silica powder peak overlaps Neat fabric at 1070 cm^{-1}, as shown in the Figure 25.

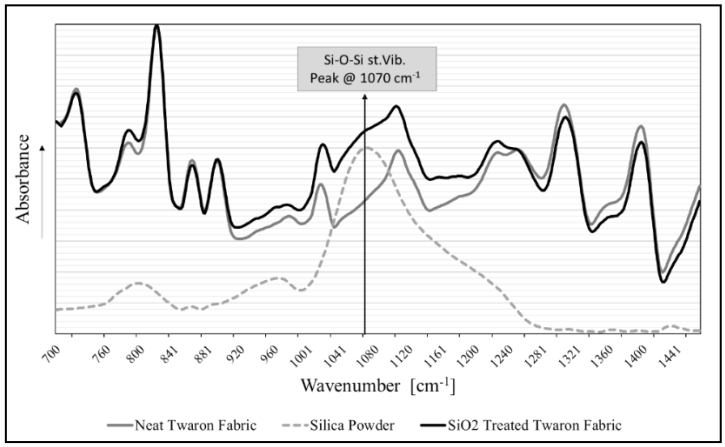

Figure 25: FTIR spectra of untreated and treated samples and silica powder

5.3.3. EDX Analysis

The atomic composition of treated and untreated surfaces was determined by EDX analysis. The peaks of the detected elements can be found in Figure 26 and the percentage of different atoms partaking are given in the Table 9. The presence of Na and Si atoms were found only on treated samples while the comparative occurrence of Si and O atoms were found to be maximum on S4 samples and concentration of Na has reduced on S4 samples as compared to S3.

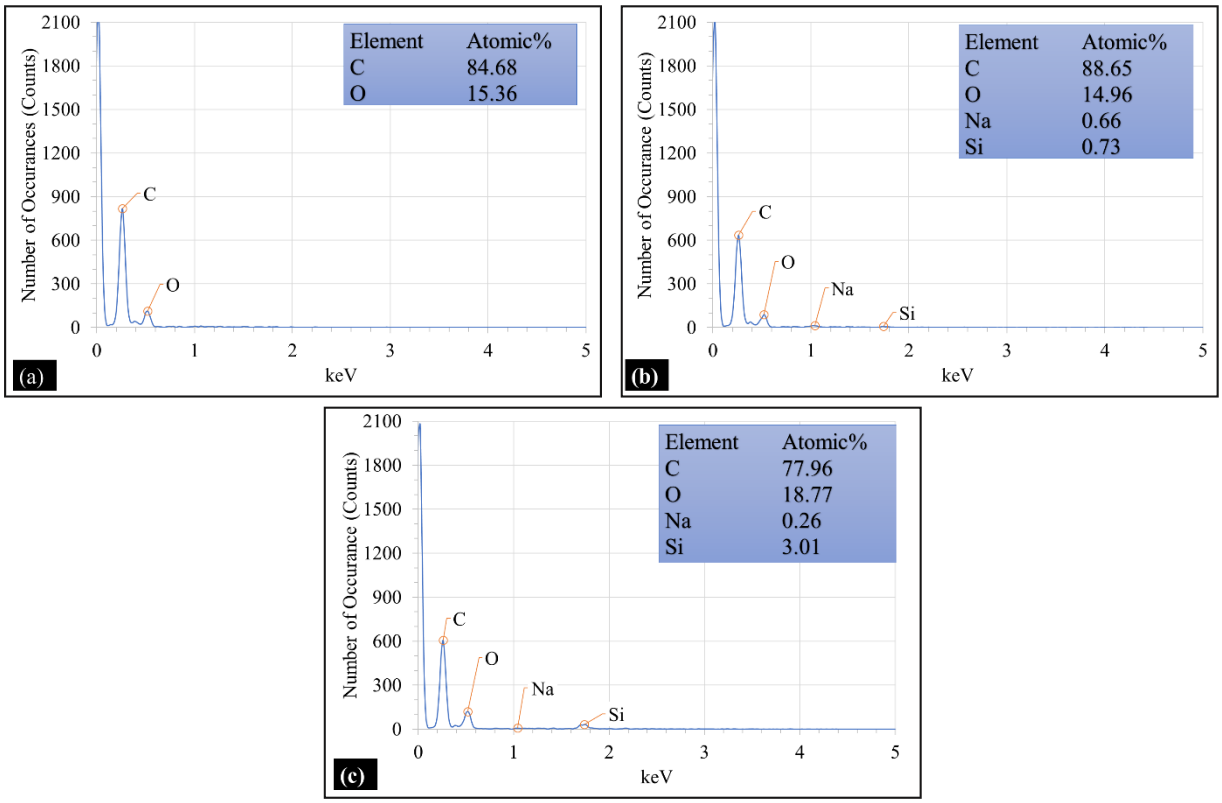

Figure 26: EDX analysis of (a) Neat, (b) S3 and (c) S4 samples.

Table 9 Element Analysis by EDX

Fabrics	Atomic (%)			
	C	O	Na	Si
N	84.64	15.36	-	-
S3	83.65	14.96	0.66	0.73
S4	77.96	18.77	0.26	3.01

The evidences obtained from SEM, FTIR and EDX analysis confirm the deposition of SiO_2 on the surface of treated samples, that can be summarised as:

1. The physical presence of the deposited layer is observable in SEM images,
2. The presence of Si-O stretch vibration peaks in FTIR spectroscopy curves and
3. The presence of Si, O and Na atoms as evident by EDX.

5.4. Change in surface friction

The coefficient of surface friction of different samples was also analysed, and the results are given in Table 10. The values in parenthesis show the Student's t-Distribution at 95% confidence interval. The coefficient of friction is found to be increased in order of

S4>2ZS4>S3>N. It may indicate that the deposition of SiO_2 causes the surface to become irregular and coarser and hence resulting in the higher coefficient of friction for fabric surface. Furthermore, a greater amount of deposition of SiO_2 on treated samples resulted in a greater increase in frictional coefficient (as evident from Table 10).

Table 10: Coefficient of friction of different fabrics

Fabrics Type	**Neat**	**S3**	**S4**	**2ZS4**
Average Coefficient of Friction, μ_s	0.24(0.02)	0.26(0.02)	0.31(0.02)	0.30(0.01)

5.4.1. The effect of surface friction changes on QSKPR:

The comparison of QSKPR force of treated and untreated samples at different penetration angles is expressed in Figure 27. The error bars represent the Student's t-Distribution at 95% confidence interval. The mean values of each fabric tested at all selected angles are represented with the horizontal line.

The bar chart establishes the statistically significant increase in penetration resistance, in the order of S4>2ZS4>S3>N. There is more than two-fold increase in mean penetration resistance from 11.88 *N* for Neat fabric to 25.55 *N* for S4 fabric. The reason of this behaviour may be due increase in frictional coefficients of treated samples which resulted in the higher knife penetration resistance. The key observations of the Neat fabric failure against the knife penetration were yarn to yarn sliding, lack of fibres gripping and partial yarn cutting. This may be reasoned to the open-structure of fabric, lack of fibre binding forces and lack of warp-weft friction. However, the behaviour of S4 sample was changed, where failure occurred due to the individual yarn cutting in one or fewer steps without yarn slippage. It may be associated with the increase in friction and knife load distribution to the neighbouring yarns. Comparison of force-displacement curves of Neat and S4 samples indicate this behaviour, as presented in Figure 28.

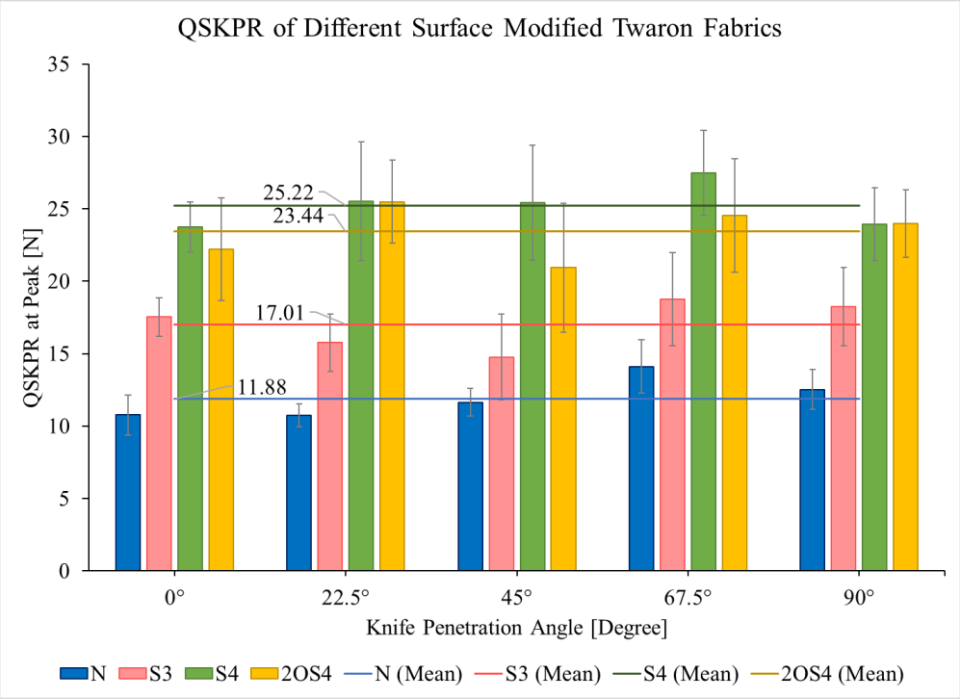

Figure 27: QSKPR of different surface modified fabrics

Close observation of the force-displacement curves discloses two facts:

1. Total numbers of peaks have reduced, for full penetration of 42 *mm*.

2. Peaks for S4 sample were relatively higher than Neat fabric, which can be related to more yarns responding simultaneously i.e. more load distribution from single yarn to neighbouring yarns because of reduced yarn slippage.

These phenomena are evident in cases when the knife does not cut the warp or weft normally i.e. in cases of penetration angles of 22.5°, 45°, and 67.5°. For other cases, at the penetration angles 0° and 90°, the number of peaks for S2 and Neat samples are same. Sparse density of yarns causes individual yarn presentation to the knife sharp edge.

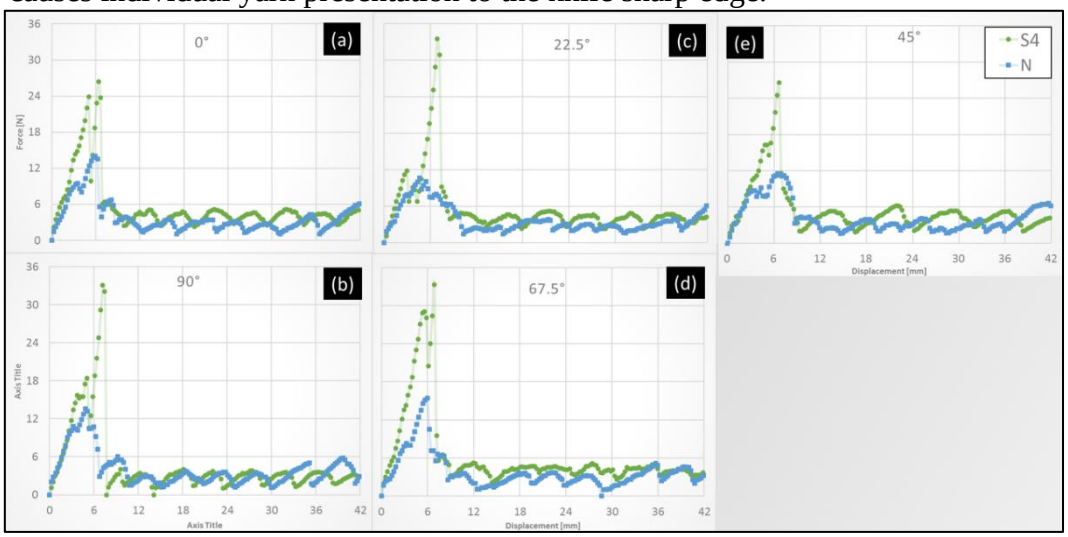

Figure 28: Force-displacement curves of Neat and S4 samples at different knife penetration angles (best of various samples)

5.4.2. The Relation of QSKPR with the amount of deposition and friction

Another analysis made from Figure 27 is that the QSKPR increases linearly with the increase in amount of SiO_2 deposition on the fabric surface. This is true for all the penetration angles. In the similar manner, it is also found that the QSKPR is related to fabric surface friction. To investigate the relation, mean surface frictions were plotted against mean QSKPR for Neat, S3 and S4 samples, as shown in the Figure 29. It is clear there is a strong dependence of variable R_{st} (QSKPR) on the independent variable μ_s (coefficient of surface friction). So, for the given amount of SiO_2 deposited in this study, it can be stated that:

$$R_{st} = f(\mu_s) \quad (1)$$

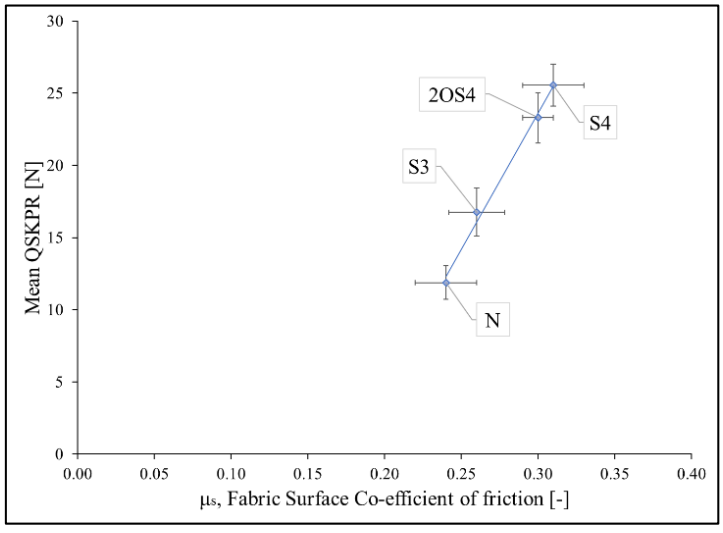

Figure 29: Effect of change of surface friction on QSKPR

1st degree polynomial linear model fitted, is shown in equation (2) and the coefficients of the model and goodness of fit of this model are shown in Table 11.

$$f(x) = p_1 x + p_2 \quad (2)$$

Table 11: QSKPR vs Fabric Friction fitted model coefficients and goodness of fit

Coefficients of Model (95% confidence bounds)	p_1		p_2	
	188.1 (142.9, 233.4)		-32.84 (-45.46, -20.22)	
Goodness of fit	**SSE**	**R-square**	**Adjusted R-sq.**	**RMSE**
	0.724	0.9938	0.9907	0.6017

5.5. The effect of KPA on QSKPR

The effect of the penetration angle on QSKPR is presented in Figure 27. The Neat fabric shows the increase QSKPR with the increase in penetration angle from 0° to 90°, with the highest resistance at 67.5° penetration angle. The similar behaviour is observed for the surface modified fabrics.

However, it should be noted that the higher penetration resistance at the 67.5° penetration angle is not statistically significantly different, for any fabric type. Only for Neat fabric, the penetration resistance for this angle is statistically significantly different from the means all Neat samples (as seen horizontal blue line in Figure 27). This analysis was performed for t-distribution test at 95% confidence level and given in Table 12. Moreover, all fabrics show comparatively higher penetration resistance at 67.5° KPA as is evident in Figure 27 except 2ZS4.

Table 12 Analysis of Variance (ANOVA) for QSKPR of Neat fabric at 67.5°

Angle	***Neat fabrics mean resistance***	***Mean resistance at 67.5°***	***P***
67.5°	11.88	14.1(12.25, 15.95)	0.017

5.5.1. Orientation of yarns at different penetration angles

The differences between the penetration resistance forces at different penetration angles can be linked to the orientation and availability of yarns to the knife edge. In Figure 30(a), the knife edge travelling at different penetration angles are shown with dotted lines. There can be three possibilities with respect to the knife travel (tr) for each consecutive yarn cutting:

1. At penetration angles 0° and 90°, one direction yarns, either wefts or warps are cut, and knife travels a distance equal to one pick spacing, denoted here with 'p', as shown in Figure 30(b) as t_0 and t_{90}. This distance is the smallest of three cases but as compared to knife travel, the warp and weft density is sparse, and the knife edge does not face consistent resistance from fabric. This is the reason that the QSKPR drops to zero after each yarn cutting, before the next yarn starts resistance against knife, as evident in Figure 28(a) and Figure 28(b).
2. For 45° penetration angle as seen in Figure 30(c), the knife engages warp and weft in orthogonal pairs. The distance travelled is √2p for each next pair. This is the maximum distance for all three cases. Also, yarn to yarn slippage is highest among all cases. That is the reason, QSKPR force-displacement curves shows higher numbers of peaks, and relatively least resistance is observed at 45°. And in the case of higher yarn to yarn friction, as in S4, the number of smaller peaks has reduced, as evident in Figure 28(e).

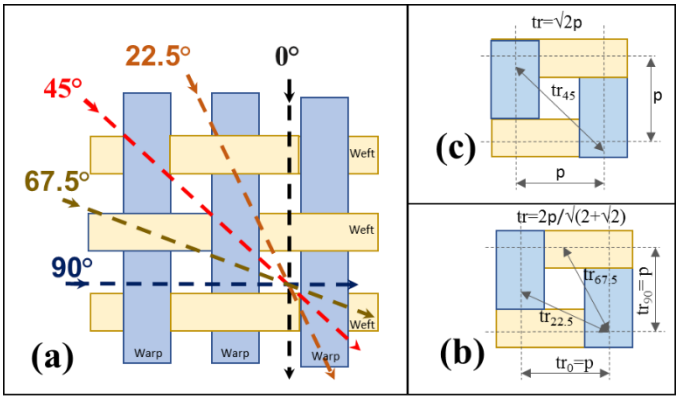

Figure 30: (a) Illustration of the path, knife edge travels at different KPA, (b) yarn to yarn distance and knife travel (t) at 0°, 90°, 22.5° and 67.5° and (c) at 45°

3. In the case of 22.5° and 67.5° penetration angles the knife edge travels a distance of $\frac{2p}{\sqrt{2+\sqrt{2}}}$, as clear in Figure 30(b), that is nearly equal to one pick spacing, 1.083p. And both warp and weft yarns offer the resistance simultaneously, although more resistance is offered by yarn that is cut near to its transverse direction. The knife travelling finds less gaps and relatively more steady fabric response is exhibited as is evident from QSKPR force-displacement curves, apparent by fewer peaks and less bumps as shown in Figure 28(c) and Figure 28(d).

The dominated higher resistance at 67.5° as compared to 22.5° and at 90° than 0° angles may be linked to the higher mechanical strength of warp yarns.

The distance knife should travel for each penetration angle is negatively relating the QSKPR, that can be expressed as:

$$R_{st} = f\left(\frac{1}{tr}\right) \quad (3)$$

5.5.2. Warp and Weft complementary cutting behaviour

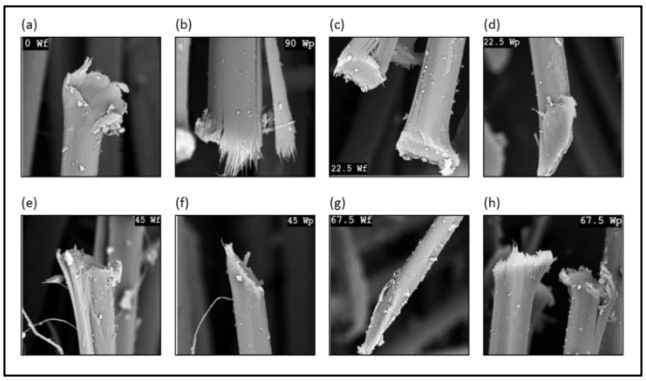

Figure 31: SEM images of fibres removed from post-penetrated fabric samples.

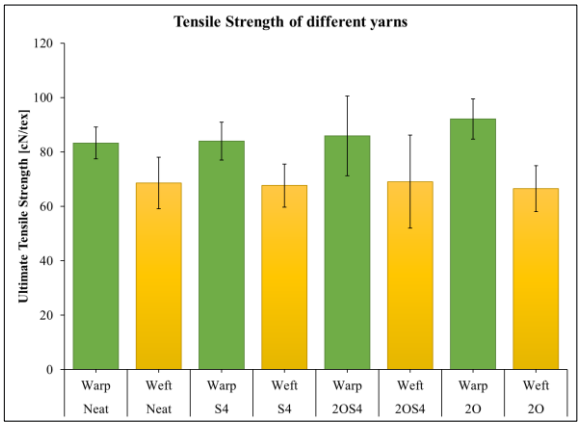

Figure 32: Comparison of the ultimate tensile strength of warp and weft yarns, removed from respective fabric

There seems to be the complementary response of warp and weft when penetration angle changes. This is also supported by the post-penetration fibre damage analysis, removed from damaged Neat fabric samples (Figure 31). It was observed that transverse knife penetration caused maximum load sharing as evident from plastic deformation at 0° and 90° penetration angles, as given in Figure 31(a) and Figure 31(b). Since warp yarns are also showing cracking,

fibrillation and fibre rupture along the length, which may be attributed to higher stress at break of warp yarns than weft yarns. This finding is supported by the fact that the tensile strength exhibited by warp yarns, of any fabric, is higher from their respective weft yarns. The ultimate tensile strength of yarns removed from different fabrics is shown in Figure 32. The an-isotropic cutting behaviour of textile fibres and yarns is already recorders [30], [32], and it is known that woven fabric show anisotropy for their mechanical characteristics, when examined at off-axis from warp or weft directions.[59]

For all the other cases the tip of damaged warp and weft yarns is in accordance with the angle at which knife cut the respective warp or weft yarn. The fibre that is cut at an angle closer to the transverse direction, shows higher plastic deformation, cracking and fibrillation. When the cutting angle decreases to lower penetration angles, a clear sharp edge is observed at the tip of the damaged fibre and plastic deformation mechanisms also diminish.

The orthogonal orientation of warp and weft makes the QSKPR complementary to 90° i.e. the sum of cut angles of warp and weft fibre is 90°. So, the fibres cutting at the smaller angle contribute less resistance than cutting at the higher angle. When yarns with the higher tensile strength are cut at higher angle, more QSKPR is exhibited. This angle dependence of QSKPR can be written as: [60]

$$R_{st(warp)} = f(\sigma_{warp} sin\alpha) \quad (4)$$

$$R_{st(weft)} = f(\sigma_{weft} sin\beta) \quad (5)$$

Considering orthogonal orientation of warp and weft:

$$\angle\alpha \perp \angle\beta$$
$$\Rightarrow sin\beta = cos\alpha$$

Therefore, the equation (5) becomes:

$$R_{st(weft)} = f(\sigma_{weft} cos\alpha) \quad (6)$$

For fabric response, combining equation (4) and (6):

$$R_{st} = R_{st(warp)} + R_{st(weft)}$$

$$R_{st} = f\left((\sigma_{warp}\, sin(\alpha)) + (\sigma_{weft}\, cos(\alpha))\right) \quad (7)$$

Here, R_{st} is QSKPR measured in *N*, σ_{warp} and σ_{weft} are the warp and weft ultimate tensile strength in measured in *cN/tex* and α is the knife penetration angle in degrees.

5.6. Video Analysis

To understand the interaction of knife and fabric the video of knife penetration, during quasi-static stab testing, was captured on CCD camera. The method and setup followed can be found in section 4.2.2.2. For comparison Neat and S4 fabric samples are analysed at 0° KPA.

The force-displacement curves are shown for Neat fabric in Figure 33 and for S4 fabric in Figure 35. These curves are labelled at different points mentioning fracture of certain yarns as numbered in Figure 34 for Neat fabric and in Figure 35 for S4 fabric.

The knife penetration can be viewed in two parts, first yarn is fracturing on blunt side and second sharp side of the knife. The yarn fracture on both sides are discussed below.

5.6.1. Blunt side yarn fracture

In both cases, of Neat and S4, as the knife starts to penetrate, the yarns interacting with blunt side of the knife are pushed aside, resulting a force like yarn pull out unless they are fractured. It is observable for yarn number 4 in Figure 34(B)-(D) and for yarn number 3 in Figure 36(B)-(D). After completion of first 6mm of knife penetration the blunt side get parallel to the length of knife, so further pressure from blunt side ends and only sharp side causes the pressure and yarn fracture. This initial fracture of yarn on blunt side is the major cause of higher peak in force-displacement curve.

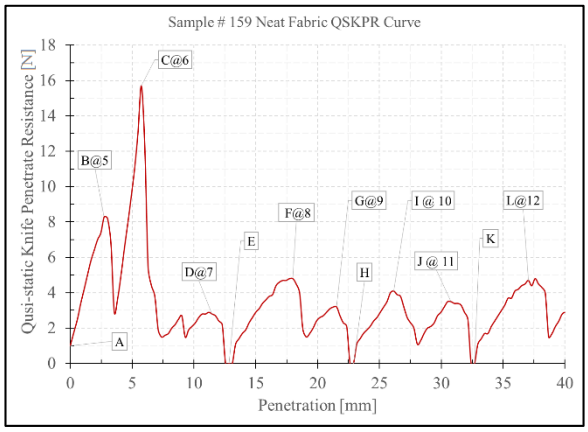

Figure 33: Force-Displacement curve for Neat fabric at 0° KPA, label pointing fracture of different yarns

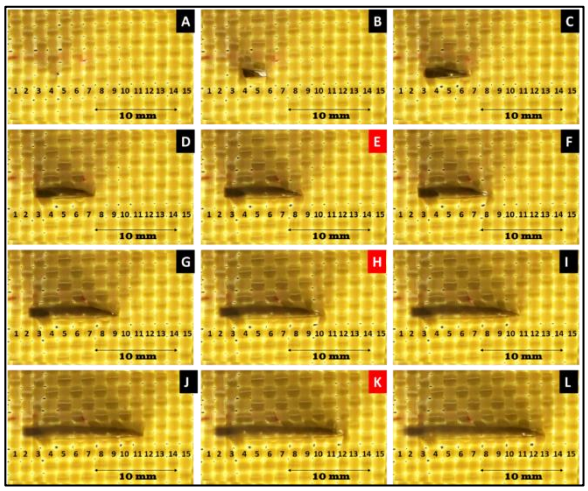

Figure 34: Camera images showing knife penetration for Neat fabric at 0° KPA, different yarn fractures are labelled, at E, H and K knife penetrates without yarn fracture.

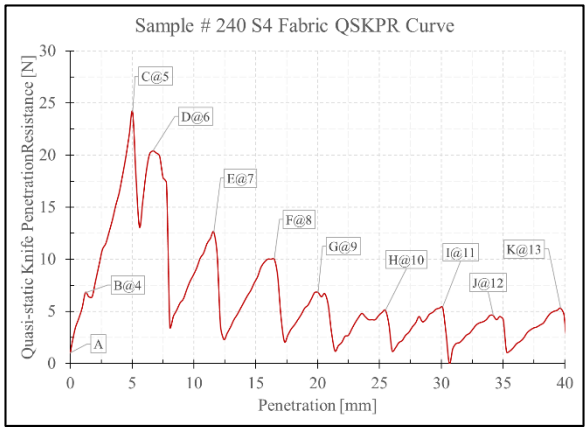

Figure 35: Force-Displacement curve for S4 fabric at 0 KPA, showing point of different yarns fracture

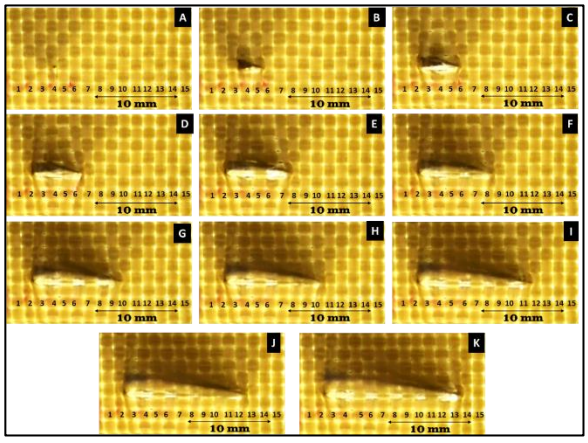

Figure 36: Camera images showing knife penetration for S4 at 0° KPA, different yarn fractures are labelled.

5.6.2. Sharp side yarn fracture

In Figure 33 and Figure 35 every peak is labelled with corresponding sub-figure and yarn number found in Figure 34 and Figure 36, respectively for Neat and S4 fabrics. Each peak is produced exactly before fracture of corresponding yarn. It can be seen that the fabric resistance falls to zero due to the gaps between yarns, for Neat fabric as mentioned at E, H and K in Figure 33 and Figure 34. While, for S4 fabric knife does not find a gap enough that resistance falls to zero. Moreover, the force-displacement curve's contours for Neat fabric are depicting inconsistent resistance from each individual yarn cutting, i.e. partial cutting of yarn which is also evident in recorded videos.

On the contrary the S4 yarn fracturing curves making clear peaks, as seen in Figure 35 at label C, D, E, F and G, that indicates the strong resistance offered by S4 individual yarns and

complete yarn cut in one step without any partial cutting. This behaviour shows the intra-fibre cohesion that make filaments of the yarn behave as single assembly.

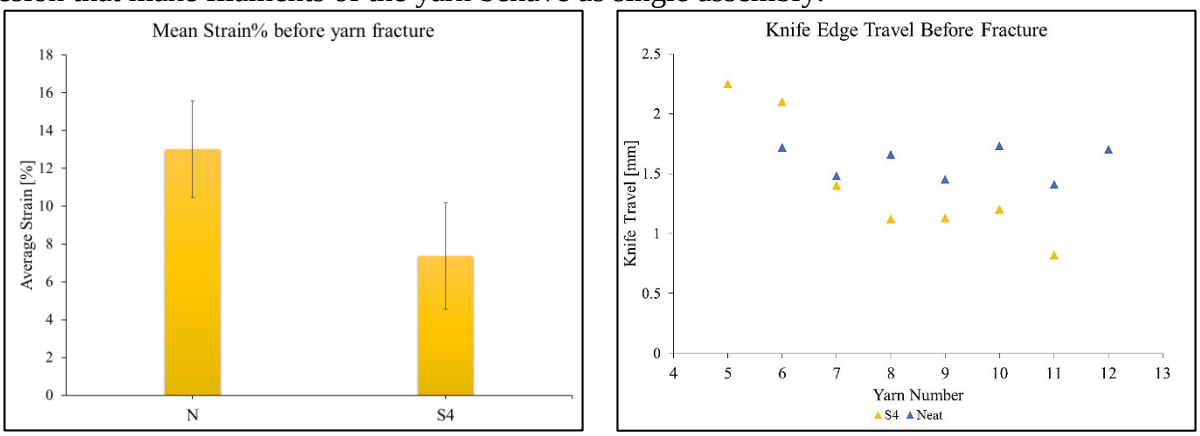

(a) (b)

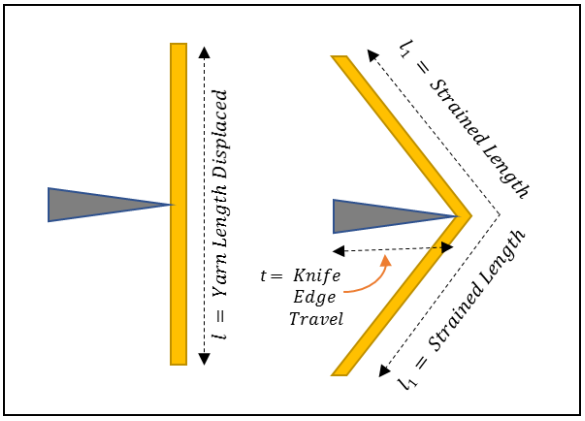

(c)

Figure 37: (a) Mean Strain % of S4 and N compute from image analysis, (b) Travel of knife edge before each yarn rupture and (c) Illustration of yarn strain before fracture

$$l_1 = \sqrt{\left(\frac{l}{2}\right)^2 + t^2} \tag{8}$$

$$Strain\ \% = \frac{(2l_1 - l)100}{l} \tag{9}$$

The other reason of higher peak of S4 than Neat is the stiffer yarn behaviour of S4 yarns. The image analysis performed for the image-frames extracted from recorded video, as shown in Figure 37(c), proves this finding. Mean strain measured (by Equation (8) and (9)) at rupture of S4 yarns was found to be lower than Neat yarns, as shown in Figure 37(a). Furthermore, the absorption of energy is higher for preceding yarns than following yarns, in case of S4 as shown for yarn number 5 and 6 in Figure 37(b).

5.7. Cutting Resistance of Individual Yarns

To examine how yarns behaviour against knife blade when no interlacement is there like in the fabric. The warp and weft yarns were removed from the treated and untreated fabrics. Their resistance against same (K1) knife edge was recorded as was used to penetrate the fabric. The details of device and procedure are already discussed in section 4.2.4.3.

The mean cutting resistance and energy versus knife vertical displacement and knife edge displacement was recorded for 10 yarns. The results are shown for Neat warp in Figure 38 and S4 warp in Figure 39. Few things are noteworthy here:

1. Near about all yarn are completely fractured for same knife displacement, similar cut resistance and cut energy.
2. Both Neat (warp and weft) yarns and few S4 weft show partial fracture, Neat yarn around midway of complete fracture displacement at around 5 *mJ* cut energy and S4 weft later than midway at around 12 *mJ*.
3. S4 warp does not show partial fracture but cut in one go. And fracture of complete yarn completes earlier than Neat yarns, for both S4 warp and weft.

These results are summarized in Table 13.

Table 13: Individual Yarn Cutting Statistics

Fabrics	Mean Cutting Resistance	Values at Peak Resistance for:		
		Yarn Cutting Energy	Knife Edge Displacement	Knife Length Displacement
	[N]	[mJ]	[mm]	[mm]
Neat Warp	2.48 (0.13)	17.75	16.78	46.1
Neat Weft	2.58 (0.19)	18.83	16.31	44.8
S4 Warp	2.54 (0.17)	18.94	14.70	40.4
S4 Weft	2.46 (0.23)	17.17	14.89	40.9

From these results it can be inferred that S4 yarns have developed enough inter-fibre cohesion that they persist partial yarn fracture to larger extent, than Neat yarns, but once cutting starts complete yarn cuts in one step. While Neat yarn individual filament resist against separately and yarns fracture by parts, showing absence of inter-fibre cohesive force.

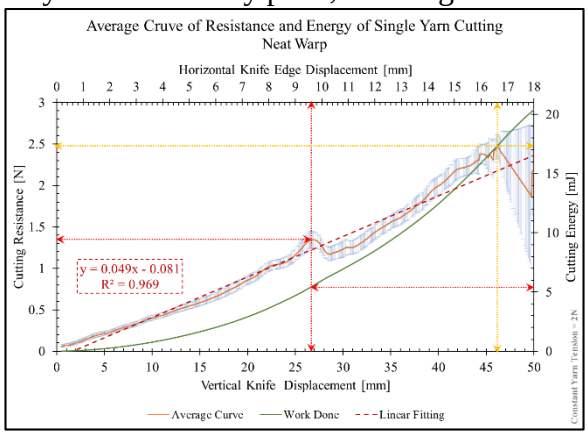

Figure 38: Mean curve for cutting resistance and cutting energy verses vertical and knife edge displacement for Neat warp

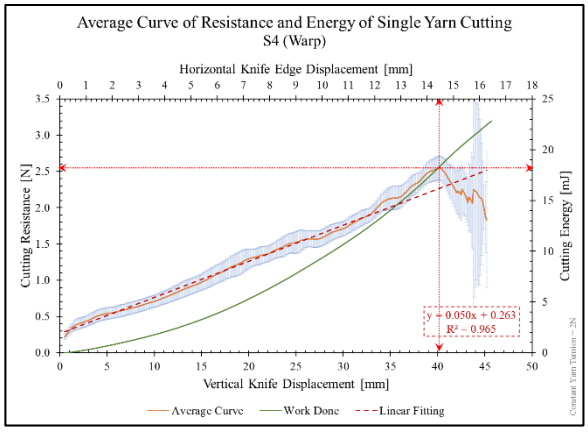

Figure 39: Mean curve for cutting resistance and cutting energy verses vertical and knife edge displacement for S4 warp

5.8. Yarn pull out force

The force required to pull out yarn from the fabric can give an estimate of friction due to yarn to yarn sliding. Yarn pull out force was measured for warp and weft of Neat and S4 fabrics following the procedure as described in section 4.2.4.2.

Each yarn was pulled out for a total of 40 interlacement. For each interlacement yarn get lose and tight as free end passes over different interlacements, this is evident from pull out data shown in Figure 40. The peaks, from yarn pull out (force-displacement) data, were plotted as

shown in Figure 41. These points were fitted with linear regression 2nd order polynomial, as found in Equation (10), the Table 14 contains the coefficient of fitted model and Table 15 shows the goodness of fit and analysis of variance. Mean pull-out resistance was computed for every peak in measurement curve by dividing the interlacements contributing to the resistance. Then mean for every fabric direction was computed and shown in Table 16.

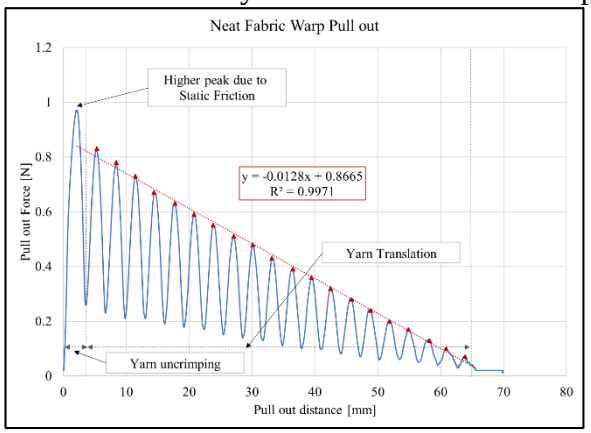

Figure 40: Force-displacement curve of Yarn Pull-out test

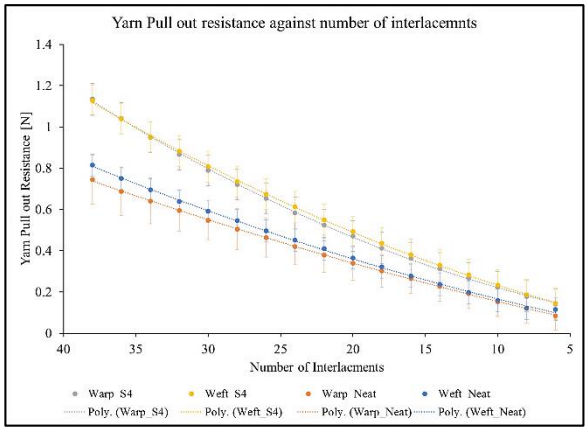

Figure 41: Yarn Pull-out resistance against opposing interlacements of yarns for warp and weft of Neat and S4 fabrics

$$f(x) = p_1x^2 + p_2x + p_3 \quad (10)$$

Table 14: Yarn pull-out coefficients of fitted models

Fabric	***Pull-out direction***	***Equation Coefficients***		
		p_1	p_2	p_3
Neat	Weft	0.000197 (0.000042)	0.0135 (0.0019)	0.0115 (0.01837)
	Warp	0.000128 (0.000016)	0.0147 (0.0007)	-0.0055 (0.00723)
S4	Weft	0.000332 (0.000029)	0.0157 (0.0013)	0.0429 (0.01279)
	Warp	0.000436 (0.000035)	0.0114 (0.0016)	0.0638 (0.01561)

Table 15: Goodness of fit 2nd degree polynomial fit

Fabric	***Pull-out direction***	***SSE***	***R-Square***	***Degree of freedom***	***Adj. R-sq.***	***RMSE***	***# Coef.***
Neat	Weft	6.55E-04	0.999189	14	0.999073	0.006838	3
	Warp	1.01E-04	0.99985	14	0.999829	0.002691	3
S4	Weft	3.17E-04	0.99979	14	0.99976	0.004758	3
	Warp	4.73E-04	0.999694	14	0.999651	0.00581	3

S4 warp and weft show significantly higher mean resistance than Neat warp and weft. Weft of both fabrics shows slightly higher resistance than respective warp, which may be related to higher crimp of weft than warp.

Table 16: Mean pull-out resistance of each interlacement

Fabric	**Pull-out Force per interlacement, [N]**	
	Warp	**Weft**
Neat	0.0172 (0.0008)	0.0185 (0.0009)
S4	0.0248 (0.0013)	0.0255 (0.0011)

5.9. Yarn Sliding Resistance

In the video analysis it was observed that on average each yarn is displaced from 1-2 *mm* before it was cut by sharp edge of the knife, sliding over opposing yarns. Once this sliding resistance is known we can observe how it is contributing to the stab resistance of the fabric.
We can measure the resistance offered by the yarns of the fabric when they slide over opposite yarns. To measure this sliding resistance a setup was designed using a thin wire as photographed in Figure 42 and the procedure explanation is given in section 4.2.4.4. The results are shown in Figure 43, for warp and weft yarns of Neat and S4 fabrics.

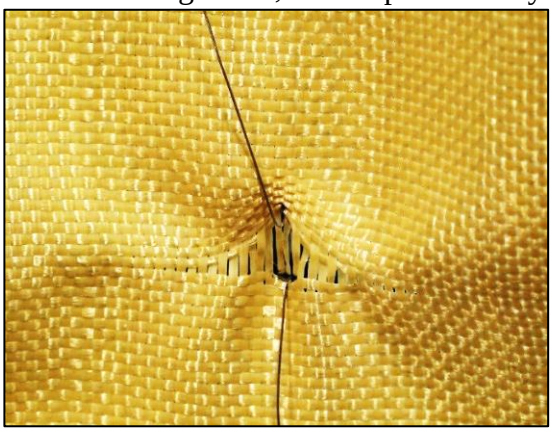

Figure 42: Fabric samples installed on Universal Testing Machine, yarn sliding resistance measurement.

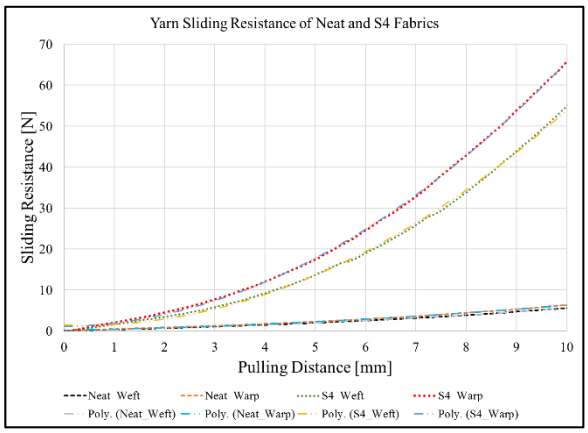

Figure 43: Fabric Sliding resistance, measured using wire loop pull up, in warp and weft direction of Neat and S4 fabrics

The sliding resistance for 10 *mm* was recorded for warp and weft of Neat and S4 fabrics, for 10 samples each. The interpolated mean values were plotted. This data was fitted with second degree polynomial (as in Equation (10) and mean resistance at 1 and 2 *mm* is shown in Table 17. The coefficient of fitted model, analysis of variance and goodness of fitted data are shown in Table 18 and Table 19.

Table 17: Yarn sliding resistance for different fabric in warp and weft direction

Fabric sliding resistance (N)					
Fabric	**Direction**	**Warp**		**Weft**	
	Sliding Distance	**1 mm**	**2 mm**	**1 mm**	**2 mm**
Neat		0.51	0.89	0.39	0.71
S4		2.17	4.58	1.68	3.48

Table 18: Parameters of fitted model

Fabric	***Equation Parameters***		
	p_1	p_2	p_3
Neat Warp	0.623 (0.0048)	0.225 (0.0498)	1.12 (0.108)
Neat Weft	0.562 (0.0073)	-0.374 (0.075)	1.439 (0.163)
S4 Warp	0.038 (0.00075)	0.231 (0.0078)	0.207 (0.0168)
S4 Weft	0.033 (0.00051)	0.211 (0.0053)	0.131 (0.0114)

Table 19: Goodness of fit for 2nd degree polynomial fitted model for slide resistance of different fabrics

Fabric	***SEE***	***R-Sq.***	***df***	***Adj. R-Sq.***	***RMSE***	***# Coef.***
Neat Warp	37.678	0.999	332	0.999	0.337	3
Neat Weft	85.633	0.999	332	0.999	0.508	3
S4 Warp	0.914	0.999	332	0.999	0.052	3
S4 Weft	0.421	0.999	332	0.999	0.036	3

5.10. Effect of Layers orientation

The minimum requirement of penetration energy defined by stab resistance standard (NIJ Standard–0115.00) cannot be fulfilled by single layer of Neat fabric. Also, stab resistant textile must have sufficient thickness to resist against stab. Therefore, multiple-sheet textile was required. Since orientation of fabric with respect to knife changes for each stack when more than one sheet is stacked at different stacking angle (SA). Therefore, stacking angle was studied for two-layered textile. Stacking angle is the angle between warp direction of two consecutive layers.

Three different SA 0°, 90° and 45° were analysed for Neat fabric samples. The orientation of different stacking angles is shown in Figure 44. Each of this orientation was tested for QSKPR in five KPAs i.e. 0°, 22.5°, 45°, 67.5° and 90°.

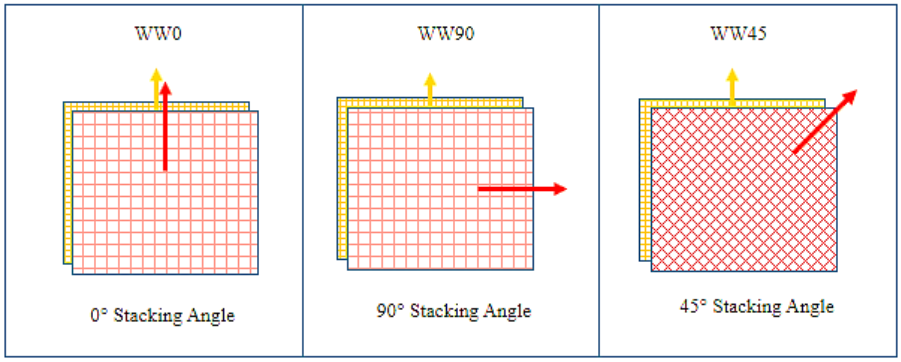

Figure 44: Stacking of two sheets at different stacking angles, arrows representing warp direction of respective fabric

5.10.1. Effect of Stacking

The QSKPR of different combinations of stacks is shown in Figure 45 and penetration energy in Figure 46. The mean QSKPR and mean Penetration Energy are represented by horizontal lines in each case. A comparison with Figure 27 discloses the fact that mean QSKPR of two sheets stack has arisen from 7 to 10 *times* than mean QSKPR of single sheet. This evident the synergic effect of multi-sheet stack.

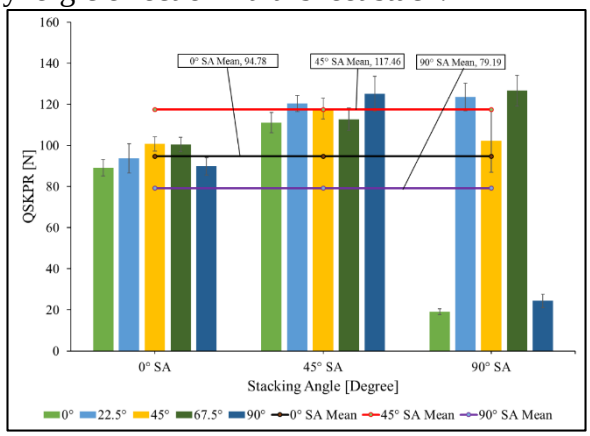

Figure 45: Change in QSKPR of different fabrics with different Stacking Angles at different KPAs

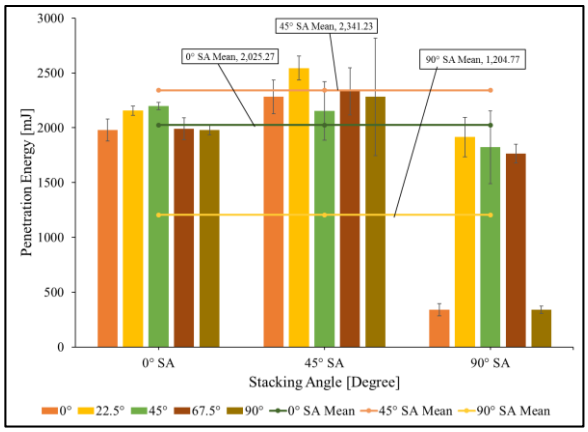

Figure 46: Change in Penetration Energy of fabrics with different Stacking Angles at different KPAs

5.10.2. Effect of Stacking Angle and KPA on QSKPR and PE

It is clear from these figures (Figure 45 and Figure 46) that change in SAs and KPAs is causing variation in QSKPR of different stacks. The error bars representing 95% confidence limits of each KPA examined. For definite understanding one-way analysis of variance (ANOVA) was performed, shown in Figure 45 and Figure 46. In all the cases F-statistics is higher than critical

F value establishing statistically significantly different mean QSKPR for each KPA examined, within each stack orientation. That confirms the change of QSKPR with varying KPA for two-sheets stack.

Table 20: One-way ANOVA for QSKPR for different SA

SA	*Source of Variation*	*SS*	*df*	*MS*	*F*	*P-value*	*F-critical*
0°	Between Groups	748.31	4	187.08	5.50	0.003	2.76
	Within Groups	849.73	25	33.99			
	Total	1598.05	29				
45°	Between Groups	644.35	4	161.09	3.05	0.035	2.76
	Within Groups	1318.75	25	52.75			
	Total	1963.10	29				
90°	Between Groups	68261.87	4	17065.47	125.53	3.641E-16	2.76
	Within Groups	3398.72	25	135.95			
	Total	71660.59	29				

The mean QSKPR of different stacks is in increasing order from 90° < 0° < 45°. To explain this order, we must consider the orientation of warp and weft yarns in different sheets of a stack. The warp and weft of two sheets are found to be aligned as illustrated in Figure 47. In earlier discussion, we have seen that the QSKPR of fabric is a complementary response (section 5.5.2) and warp dominates in load bearing. This trend has been magnified when warps of both sheets are aligned, as in case of SA of 0°, shown in Figure 47(a). If we compare the single sheet QSKPR of Neat fabric (Figure 27) and two-sheets stack results (Figure 45) a resemblance can be found for response at different KPAs.

In case of SA of 90° the warp of two sheets aligned perpendicular to each other, as shown in Figure 47(c) and that may be the reason of loss of QSKPR at 0° and 90° KPAs, at this SA. That is, when knife is penetrating parallel, to warps of one of the sheets, the stabbing resistance achieved is like as achieved by single sheet QSKPR. Also, when knife is not penetrating parallel to the warp direction of any sheet the strength exhibited is comparable to QSKPR shown at SA 0° or 45°.

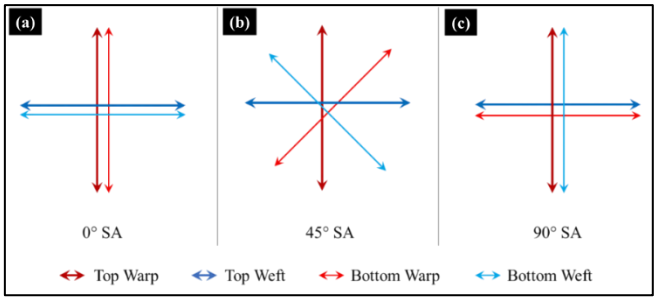

Figure 47: Orientation of warps and wefts for different sheets at different SAs

For the case of 45° SA mean QSKPR is found to be maximum in comparison to other SAs. Similar reason, as discussed earlier, is found to be present in this case also. The knife gets parallel to the yarns of one direction at 0°, 45° or 90° KPA, present in any one of the sheets. KPA is measured from the top sheet that come first in contact with knife. At 45° KPA warp or weft of the bottom sheet is parallel to knife. In the case of warp, the QSKPR may reduce and in case of weft it may not reduce to that extent. That is the reason of much variation of PE at 45° KPA for 45° SA. Similarly, at 0° KPA warp of the top sheet and at 90° KPA weft of the top sheet is parallel to penetrating knife i.e. QSKPR and PE is achieved as is evident from the bar charts, in Figure 45 and Figure 46. For the other two KPAs (i.e. 22.5° and 67.5°), we observe maximum PE and comparable QSKPR because no yarn is parallel to knife and cutting

energy is distributed among all the yarns of both sheets leading to the best PE and one of the best QSKPR of all the results observed.
From all these discussions, it can be safe to infer that more the number of yarns resisting in multiple directions, for various sheets of stack, higher will be the distribution of stabbing energy and more resistance is offered by the textile.

5.11. Dynamic Stab Resistance (DSR)

The best result of QSKPR‹ in double sheet stack‹ was found for 45° SA. So, 45° SA was chosen for dynamic stab testing. Warp of each next sheet was turned 45° from warp of next sheet, for 8 sheets stack. The drop-tower was used to drop knife, under gravity, on to the fabric samples, mounted on backing material. The procedure is described in section 4.2.2.3. The sample being tested was tapped with backing material platform and it was rotated to allow knife drop in five different direction (KPAs) so that knife cutting axis make 0°, 22.5°, 45°, 67.5° or 90° with warp of the top most sheet.
The penetration depth was recorded by the machine and was also confirmed from cut produced in the paper sheets placed in backing material. The mean of penetration depth recorded for all KPAs is presented in Figure 48. Two penetration energies were examined.
From these results it is clear that treated fabric, S4, has more stab resistance than untreated fabric for both the energies examined. Increasing the drop energy increases the depth of penetration in Neat fabric while S4 samples remain similar.

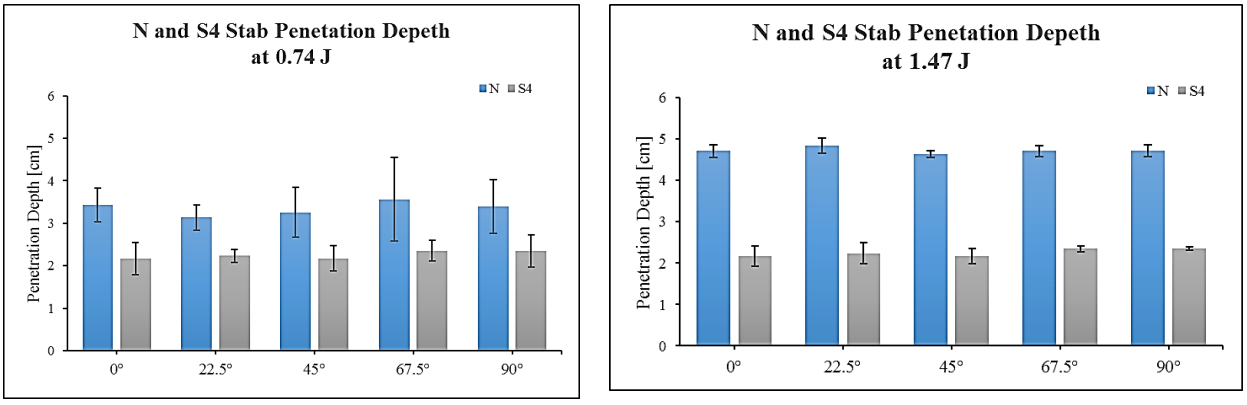

(a) (b)

Figure 48: Comparison of dynamic stab resistance in terms of knife penetration depth for Neat and S4 samples, (a) 0.74 J and (b) 1.47 J

The other observation is for both the fabrics showing no effect of KPA for both penetrated energies. This may be attributed to the SA which cause distribution of impact energy in multiple directions and hence similar response in all penetration directions was achieved. This finding supports the fact that to achieve isotropic response, from multi-sheet stab resistance textile, the stacking angle should be small enough such that, it distributes the penetration energy in multiple directions.

6. Conclusions, Applications and Future Work

6.1. Conclusions

This research investigated the quasi-static knife penetration resistance (QSKPR) and dynamic stab resistance (DSR) of single and stack of multiple sheets of woven fabric. The interaction of fabric and knife was studied when penetration was performed in different directions. The angle made between warp direction of the fabric and the knife cutting axis was called knife penetration angle (KPA). The KPA was change at five different angles i.e. 0°, 22.5°, 45°, 67.5°, and 90°. For multiple sheet stack, Stacking Angle (SA) is the angle made between warp of each consecutive sheet. For double sheet stack three SA (0°, 45°, and 90°) were investigated and

best SA (45°) was investigated for DSR of eight sheets stack. To investigate the effect of change in friction, the surface of fabric was modified with SiO_2, TiO_2 and Ozone with SiO_2. The effect of KPA and SA was investigated on QSKPR and DSR. Treated and untreated fabrics was investigated for their comfort, mechanical and physical change on their surface.

A new approach to deposit SiO_2 using water glass (WG) as precursor was discovered. Light acidic medium used helped to deposit SiO_2 on the surface of fibres. SiO_2 deposition was confirmed using Scanning Electron Microscope (SEM), Fourier Transform Infra-red (FTIR) Spectroscopy and Energy-Dispersive X-ray (EDX) Spectroscopy. The deposited layer adds weight up to 8%, fills the pores, increases inter-fibre, inter-yarn and surface friction of the fabric. Increase in the fabric friction was found to be directly proportional to the concentration of WG. Ozone application improves the tensile strength and reduces the bending rigidity. Before depositing SiO_2 layer, pre-treatment with Ozone for 120 minutes achieves the similar frictional characteristics, with better comfort. tensile strength and flexibility properties. Presence of TiO_2 on fabric surface was observed under SEM. TiO_2 particle deposited on fibre surface from its aqueous solution require binding agent to fix with fibres surface. Without binding agent, increasing concentration of aqueous solution of TiO_2 from 0.01 *g/l* to 0.5 *g/l* does not improve the stabbing performance of para-Aramid fabrics.

It was found that increasing amount of deposited SiO_2 increases the QSKPR and DSR. With 40% WG solution increase in QSKPR and DSR was found to increase about 200% for all KPAs. The response of fabric against QSKPR changed from partial yarn cutting to individual yarn cutting in fewer steps and load was distributed to larger area due to increase in inter-yarn friction and intra-yarn cohesion. The distance that cutting knife travelled for cutting consecutive yarns was changed with the change in knife penetration angle that inversely affected the QSKPR. The increase in friction of treated fabrics distributed the knife stabbing load to neighbouring yarns. This distribution was complementary between warp and weft yarns depending on knife penetration angle. The change in penetration angle changed the distribution of stabbing load among the warp and weft yarns. The higher QSKPR was resulted when the load was carried by both warp and weft yarns, at a penetration angle (67.5°) that actuated to induce more stresses in the yarns with higher tensile strength and yarn to yarn friction.

The model was developed from Fourier function for QSKPR (R_{st}) response of each fabric for various KPAs. The model fits well for all untreated and treated fabrics responses except for S4, which showed least variations in QSKPR for different KPAs. Video analysis unveiled that yarn present on blunt side of knife are fractured in yarn pull out while sharp edge of knife displaces the yarn first, sliding over other yarns, and then fracture it in parts. SiO_2 treated fabric exhibited presence of intra-yarn cohesion to persist partial yarn fracture to a larger extent than untreated yarn, that showed absence of such cohesive force. The yarns of SiO_2 treated fabric required significantly lower strain than untreated fabric, showing higher modulus of rigidity. Yarn to yarn friction was found to be higher in treated fabrics than untreated fabrics that required more pull out force or higher resistance of yarn sliding.

Stacked setup of multiple sheets produced higher response of QSKPR and DSR due to more contact area of fabrics interacting with knife and more time available to resist against the knife. Stacking also provided ability of resisting textile to distribute penetrating energy in multiple directions. Sheets stack at 45° SA was found to well distribute penetration energy and exhibit higher QSKPR and DSR and, also, improved isotropy of stab resistance.

6.2. Applications

The essence of this project can be applied to any impact resistance application for resisting against high-energy sharp-edged objects.

6.2.1. Knife stab evaluation

For knife stab testing, it is suggested that at least three cutting angles with a difference of 22.5°be examined for homogeneity of stabbing response, either from warp or weft of the woven fabric.

6.2.2. Stacking orientation

For the multiple-sheets stacks required for anti-stabbing systems, each sheet in the stack must be rotated to orient yarn of different sheets at different angle i.e. 45° SA.

6.2.3. Ozone treatment and SiO_2 deposition method

The benefit of this research can be obtained by employing the deposition method developed in this work using WG as source of SiO2 deposited layer. Ozone pre-treatment before SiO_2 deposition on the fabric, can enhance the tensile strength of the yarns with lesser effect to bending rigidity and porosity as compared to untreated fabrics.

6.3. Future Work

In future, more SAs can be verified to optimize for best knife stabbing response. Upon, such knowledge a stab resistance solution may be developed.

7. References

[1] E. L. Thomas, *Opportunities in Protection Materials Science and Technology for Future Army Applications*. 2012.

[2] R. A. Scott, *Textiles for protection*. Elsevier, 2005.

[3] X. Chen, "Introduction," in *Advanced Fibrous Composite Materials for Ballistic Protection*, 2016, pp. 1–10.

[4] M. Hudspeth, W. Chen, and J. Zheng, "Why the Smith theory over-predicts instant rupture velocities during fiber transverse impact," *Text. Res. J.*, p. 0040517515586158, (2015).

[5] S. Rebouillat, "ARAMIDS: 'disruptive', open and continuous innovation," in *Advanced Fibrous Composite Materials for Ballistic Protection*, X. Chen, Ed. 2016, pp. 11–70.

[6] E. G. Chatzi and J. L. Koenig, "Morphology and structure of kevlar fibers: A review," *Polym. Plast. Technol. Eng.*, vol. 26, no. 3–4, pp. 229–270, (1987).

[7] H. S. Hwang, M. H. Malakooti, B. A. Patterson, and H. A. Sodano, "Increased interyarn friction through ZnO nanowire arrays grown on aramid fabric," *Compos. Sci. Technol.*, vol. 107, pp. 75–81, (2015).

[8] K. K. Govarthanam, S. C. Anand, and S. Rajendran, "Development of Advanced Personal Protective Equipment Fabrics for Protection Against Slashes and Pathogenic Bacteria Part 1: Development and Evaluation of Slash-resistant Garments," *J. Ind. Text.*, vol. 40, no. 2, pp. 139–155, (2010).

[9] H. Kim and I. Nam, "Stab Resisting Behavior of Polymeric Resin Reinforced p-Aramid Fabrics," *J. Appl. Polym. Sci.*, vol. 123, pp. 2733–2742, (2012).

[10] C. Eades, "Knife Crime': ineffective reactions to a distracting problem," *A Rev. Evid. policy*, vol. 1, 2006.

[11] G. Nolan, S. V. Hainsworth, and G. N. Rutty, "Forces required for a knife to penetrate a variety of clothing types," *J. Forensic Sci.*, vol. 58, no. 2, pp. 372–379, (2013).

[12] J. R. Sorensen, M. D. Cunningham, M. P. Vigen, and S. O. Woods, "Serious assaults on prison staff: A descriptive analysis," *J. Crim. Justice*, vol. 39, no. 2, pp. 143–150, (2011).

[13] M. J. Decker, C. J. Halbach, C. H. Nam, N. J. Wagner, and E. D. Wetzel, “Stab resistance of shear thickening fluid (STF)-treated fabrics,” *Compos. Sci. Technol.*, vol. 67, no. 3–4, pp. 565–578, (2007).

[14] J. Barker and C. Black, “Ballistic vests for police officers: using clothing comfort theory to analyse personal protective clothing,” *Int. J. Fash. Des. Technol. Educ.*, vol. 2, no. 2–3, pp. 59–69, (2009).

[15] H. N. Choi *et al.*, “Stab resistance of aramid fabrics reinforced with silica STF,” in *18th international conference on composite materials*, 2011, pp. 1–4.

[16] K. Bilisik, *Impact-resistant fabrics (ballistic/stabbing/slashing/spike)*. Elsevier Ltd., 2018.

[17] D. Grinevičiūtė, A. Abraitienė, A. Sankauskaitė, D. M. Tumėnienė, L. Lenkauskaitė, and R. Barauskas, “Influence of Chemical Surface Modification of Woven Fabrics on Ballistic and Stab Protection of Multilayer Packets,” *Mater. Sci.*, vol. 20, no. 2, pp. 193–197, (2014).

[18] P. V. Cavallaro, “Soft Body Armor : An Overview of Materials , Manufacturing , Testing , and Ballistic Impact Dynamics,” 2011.

[19] E. D. LaBarre *et al.*, “Effect of a carbon nanotube coating on friction and impact performance of Kevlar,” *J. Mater. Sci.*, vol. 50, no. 16, pp. 5431–5442, (2015).

[20] S. Gürgen and M. C. Kuşhan, “The stab resistance of fabrics impregnated with shear thickening fluids including various particle size of additives,” *Compos. Part A Appl. Sci. Manuf.*, vol. 94, pp. 50–60, (2017).

[21] J. A. Bencomo-Cisneros *et al.*, “Characterization of Kevlar-29 fibers by tensile tests and nanoindentation,” *J. Alloys Compd.*, vol. 536, no. SUPPL.1, pp. S456–S459, (2012).

[22] S. V Kulkarni and J. S. R. V. V Rosen, “An investigation of the compressive strength of Kevlar 49 / epoxy composites,” no. September, pp. 217–225, (1975).

[23] M. Miraftab, *Fatigue failure of textile fibres*. CRC Press, 2009.

[24] B. S. Wong and X. Wang, “Biaxial rotation fatigue in textile fibres,” in *Fatigue failure of textile fibres*, M. Miraftab, Ed. CRC Press, 2009, pp. 73–91.

[25] T. Aramid, “Ballistic materials handbook,” 2018. [Online]. Available: https://www.teijinaramid.com/wp-content/uploads/2018/03/TEIJ_Handbook_Ballistics_2018_WEB.pdf. [Accessed: 16-Sep-2018].

[26] Dupont, “Kevlar ® Reference Designs for Vests made with DuPont Kevlar XP,” 2010. [Online]. Available: http://www.dupont.com/content/dam/dupont/products-and-services/fabrics-fibers-and-nonwovens/fibers/documents/DSP_KevlarXP_ReferenceDesigns_K23338.pdf. [Accessed: 16-Sep-2018].

[27] N. Benson *et al.*, “The development of a stabbing machine for forensic textile damage analysis,” *Forensic Sci. Int.*, vol. 285, p. 161, (2018).

[28] M. Y. Yuhazri, N. H. C. H. Nadia, H. Sihombing, S. H. Yahaya, and A. Abu, “A review on flexible thermoplastic composite laminate for anti-stab applications,” *J. Adv. Manuf. Technol.*, vol. 9, no. 1, p. 28, (2015).

[29] M. D. Gilchrist, S. Keenan, M. Curtis, M. Cassidy, G. Byrne, and M. Destrade, "Measuring knife stab penetration into skin simulant using a novel biaxial tension device," *Forensic Sci. Int.*, vol. 177, no. 1, pp. 52–65, (2008).

[30] J. Mayo and E. Wetzel, "Cut resistance and failure of high-performance single fibers," *Text. Res. J.*, vol. 84, no. 12, pp. 1233–1246, (2014).

[31] B. N. Vu Thi, T. Vu-Khanh, and J. Lara, "Mechanics and mechanism of cut resistance of protective materials," *Theor. Appl. Fract. Mech.*, vol. 52, no. 1, pp. 7–13, (2009).

[32] H. S. Shin, D. C. Erlich, J. W. Simons, and D. A. Shockey, "Cut Resistance of High-strength Yarns," *Text. Res. J.*, vol. 76, no. 8, pp. 607–613, (2006).

[33] J. Mayo and E. D. Wetzel, "Cut Resistance and Fracture Toughness of High Perfomance Fibers," in *Dynamic Behavior of Materials, Volume 1*, 2011, pp. 167–173.

[34] M. Hudspeth, D. Li, J. Spatola, W. Chen, and J. Zheng, "The effects of off-axis transverse deflection loading on the failure strain of various high-performance fibers," *Text. Res. J.* , (2015).

[35] A. M. Sadegh and P. V. Cavallaro, "Mechanics of Energy Absorbability in Plain-Woven Fabrics: An Analytical Approach," *J. Eng. Fiber. Fabr.*, vol. 7, no. 1, pp. 10–25, (2012).

[36] B. J. Briscoe and F. Motamedi, "The ballistic impact characteristics of aramid fabrics: the influence of interface friction," *Wear*, vol. 158, no. 1–2, of pp. 229–247, (1992).

[37] Y. Wang, X. Chen, R. Young, and I. Kinloch, "Finite element analysis effect of inter-yarn friction on ballistic impact response of woven fabrics," *Compos. Struct.*, vol. 135, pp. 8–16, (2016).

[38] M. El Messiry and E. Eltahan, "Stab resistance of triaxial woven fabrics for soft body armor," *J. Ind. Text.*, vol. 45, no. 5, pp. 1062–1082, (2016).

[39] L. Wang, S. Zhang, W. M. Gao, and X. Wang, "FEM analysis of knife penetration through woven fabrics," *C. - Comput. Model. Eng. Sci.*, vol. 20, no. 1, pp. 11–20, (2007).

[40] J. Militký and C. Becker, "Selected Topics of Textile and Material Science," in *Selected Topics of Textile and Material Science*, D. Křemenáková, R. Mishra, J. Militký, and J. Šesták, Eds. Liberec: Publishing House of WBU, 2011, p. 404.

[41] H. S. Shin, D. C. Erlich, and D. A. Shockey, "Test for measuring cut tesistance of yarns," *J. Mater. Sci.*, vol. 38, pp. 3603–3610, (2003).

[42] X. Feng, S. Li, Y. Wang, Y. Wang, and J. Liu, "Effects of different silica particles on quasi-static stab resistant properties of fabrics impregnated with shear thickening fluids," *Mater. Des.*, vol. 64, pp. 456–461, (2014).

[43] D. B. Stojanović *et al.*, "Mechanical and anti-stabbing properties of modified thermoplastic polymers impregnated multiaxial p-aramid fabrics," *Polym. Adv. Technol.*, vol. 24, no. 8, pp. 772–776, (2013).

[44] A. Ní Annaidh, M. Cassidy, M. Curtis, M. Destrade, and M. D. Gilchrist, "A combined experimental and numerical study of stab-penetration forces," *Forensic Sci. Int.*, vol. 233, no. 1–3, pp. 7–13, (2013).

[45] W. Barnat and D. Sokołowski, "The study of stab resistance of dry aramid fabrics," *Acta Mech. Autom.*, vol. 8, no. 1, pp. 53–58, (2014).

[46] Y. Wang, X. Chen, R. Young, I. Kinloch, and G. Wells, “A numerical study of ply orientation on ballistic impact resistance of multi-ply fabric panels,” *Compos. Part B Eng.*, vol. 68, pp. 259–265, (2015).

[47] G. Angeloni, “Woven Fabric Data Sheet Gg 200 P,” p. 1, 2016.

[48] T. E. of Encyclopaedia Britannica, “Water Glass,” *The Editors of Encyclopædia Britannica*, 2014. [Online]. Available: https://www.britannica.com/science/water-glass. [Accessed: 24-Feb-2017].

[49] Y. Sun, T. Song, and W. Pang, “Synthesis of β-zeolites using water glass as the silicon source,” Sep-1996.

[50] AEROXIDE, “TiO2 P25 Hydrophilic fumed titanium dioxide Characteristic physico-chemical data,” 2014. [Online]. Available: https://www.aerosil.com/www2/uploads/productfinder/AEROXIDE-TiO2-P-25-EN.pdf. [Accessed: 20-Mar-2017].

[51] Evonik, “AEROXIDE®, AERODISP® and AEROPERL® titanium dioxide as photocatalyst,” pp. 1–12, (2013).

[52] C. Guo, L. Zhou, and J. Lv, “Effects of expandable graphite and modified ammonium polyphosphate on the flame-retardant and mechanical properties of wood flour-polypropylene composites,” *Polym. Polym. Compos.*, vol. 21, no. 7, pp. 449–456, (2013).

[53] T. T. Li, R. Wang, C. W. Lou, and J. H. Lin, “Static and dynamic puncture behaviors of compound fabrics with recycled high-performance Kevlar fibers,” *Compos. Part B Eng.*, vol. 59, pp. 60–66, (2014).

[54] R. Gadow and K. von Niessen, “Lightweight ballistic with additional stab protection made of thermally sprayed ceramic and cermet coatings on aramide fabrics,” *Int. J. Appl. Ceram. Technol.*, vol. 3, no. 4, pp. 284–292, (2006).

[55] NIST, “Stab Resistance of Personal Body Armor, NIJ Standard-0115.00,” *Stab Resist. Pers. Body Armor, NIJ Stand.*, vol. JR000235, p. , (2000).

[56] J. L. Park, B. il Yoon, J. G. Paik, and T. J. Kang, “Ballistic performance of p-aramid fabrics impregnated with shear thickening fluid; Part I – Effect of laminating sequence,” *Text. Res. J.*, vol. 82, no. 6, pp. 527–541, (2012).

[57] Y. Wang, J. Wiener, J. Militký, R. Mishra, and G. Zhu, “Ozone Effect on the Properties of Aramid Fabric,” *Autex Res. J.*, vol. 0, no. 0, (2016).

[58] S. Inoue, K. Morita, K. Asai, and H. Okamoto, “Preparation and Properties of Elastic Polyimide-Silica Composites using Silanol Sol from Water Glass,” *J. Appl. Polym. Sci.*, vol. 92, no. 4, pp. 2211–2219, (2004).

[59] N. Pan and X. Zhang, “Shear Strength of Fibrous Sheets: An Experimental Investigation,” *Text. Res. J.*, vol. 67, no. 8, pp. 593–600, (1997).

[60] M. U. Javiad, J. Militky, J. Wiener, J. Salacova, A. Jabbar, and M. Umair, “Effect of surface modification and knife penetration angle on the Quasi-Static Knife Penetration Resistance of para-aramid fabrics.,” *J. Text. Inst.*, pp 1-18, (2018)

8. Publications and CV

CURRICULUM VITAE	**Muhammad Usman Javaid** E-34/1 Street Number 1 Firdous Park, Lahore Pakistan, +420773876164, muhammad.usman.javaid@tul.cz
Education	**PhD (In progress) Technical University Liberec, Czech Republic** Major: Textile Technics and Material Engineering **MIT (2012) Virtual University, Pakistan** Major: Information Technology **BSc Engineering (2004) National Textile University, Faisalabad, Pakistan** Major: Fabric Manufacturing
Work Experience	**Lecturer (2009-Present)** Department of Fabric Manufacturing National Textile University, Faisalabad, Pakistan **Fabric Designer and Developer (2008-2009)** Zephyr Textile Limited, Lahore, Pakistan **Lecturer (2006-2008)** Department of Fabric Manufacturing National Textile University, Faisalabad, Pakistan **Assistant Weaving Manager (2004-2005)** Nishat Chunian Mills Limited, Kasur, Pakistan
Related Journal Publications	**M. U. Javaid**, et al. "Effect of surface modification of para-Aramid fabrics with Water Glass on their Quasi-Static Knife Penetration Resistance." Journal of Textile Institute, DOI:10.1080/00405000.2018.1496988
Related Conference Publications	**M. U. Javaid**, et al. "Effect of Surface Modification of Para-Aramid Fabric on Its Quasi-Static Knife Penetration (QSKP) With Water Glass and Ozone Treatments." Proceedings of workshop Billa Voda, September 2016
Other Journal Publications	• Ali, Azam, V. Baheti, **M. U. Javaid**, and J. Militky. "Enhancement in ageing and functional properties of copper-coated fabrics by subsequent electroplating" Applied Physics A, 2018 Vol. 124, No. 9, pp. 651 • M. S. Naeem, S. Javed, V. Baheti, J. Wiener, **M. U. Javaid**, S. Z. Hassan, A. Mazari, and J. Naeem. "Adsorption Kinetics of Acid Red on Activated Carbon Web Prepared from Acrylic Fibrous Waste" Fiber and Polymer, 2018 Vol. 19, No. 1, pp. 71-81

- Jabbar, J. Militky, J. Wiener, **M. U. Javaid**, and S. Rawawiire "Tensile, surface and thermal characterization of jute fibres after novel treatments" Indian Journal of Fibre & Textile Research Vol. 41, September 2016, pp. 249-254
- K. Shaker, Y. Nawab, **M. U. Javaid**, M. Umair, and M. Maqsood. "Development of 3D Woven Fabric Based Pressure Switch" AUTEX Research Journal, Vol. 15, No 2, June 2015.
- M. Maqsood, Y. Nawab, **M. U. Javaid**, K. Shaker, and M. Umair. "Development of seersucker fabrics using single warp beam and modelling of their stretch-recovery behavior" The Journal of The Textile Institute, 2015 Vol. 106, No. 11, pp. 1154–1160

Book Chapter

- A. Jabbar, J. Militky, A. Ali, **M. U. Javaid**, "Investigation of Mechanical and Thermomechanical Properties of Nanocellulose Coated Jute/Green Epoxy Composites" Advances in Natural Fiber Composites, 2018, pp. 175-194, DOI: http://doi.org/10.1007.978-3-319-664641-1_16

Conference Publications

- M. Zubair, M. Z. Ahmed, **M. U. Javaid**. "Influence of Fabric Architecture and Material on Physical Properties of 3D Multilayer Woven Fabrics.", Proceedings of 9th Central European Conference 2017, 14th September 2017, Liberec Czech Republic, pp. 135-138
- **M. U. Javaid**, et al., "Radiation distribution characterization of fluorescent dyed polyester fabrics at 633 nm wavelength.", Proceedings of workshop Svetlanka, 22-25 September 2015, pp. 73-76.
- **M. U. Javaid**, et al. "Viscose Fiber Strength and Degree of Polymerization", Conference: First International Young Engineers Convocation, At University of Engineering, Lahore, April 2014.

Research Projects

- Member of student grant competition (SGS) project 2017 titled," Development of electrically conductive textile materials (composites) for multi-functional applications", Faculty of Textile, Technical University of Liberec, Czech Republic.
- Member of student grant competition (SGS) project 2016, titled, "Nano-basalt filler nanocomposites based on natural fibers: Characterization of mechanical, impact, thermo-mechanical and fire properties.", Faculty of Textile, Technical University of Liberec, Czech Republic.
- Leader of the student grant competition (SGS) project 2015, titled, "materials for photodynamic therapy", Faculty of Textile, Technical University of Liberec, Czech Republic.

9. Record of the state doctoral exam

TECHNICKÁ UNIVERZITA V LIBERCI
Fakulta textilní

ZÁPIS O VYKONÁNÍ STÁTNÍ DOKTORSKÉ ZKOUŠKY (SDZ)

Jméno a příjmení doktoranda:	**Muhammad Usman Javaid**
Datum narození:	**2. 3. 1981**
Doktorský studijní program:	**Textilní inženýrství**
Studijní obor:	**Textile Technics and Material Engineering**
Termín konání SDZ:	**3. 10. 2017**

prospěl **neprospěl**

Komise pro SDZ:

		Podpis
Předseda:	prof. Ing. Jiří Militký, CSc.	
Místopředseda:	doc. Ing. Martin Bílek, Ph.D.	
Členové:	prof. Ing. Miroslav Václavík, CSc.	
	doc. Rajesh Mishra, Ph.D., B. Tech.	
	doc. Ing. Antonín Potěšil, CSc.	
	Ing. Brigita Kolčavová Sirková, Ph.D.	
	Ing. Blanka Tomková, Ph.D.	

V Liberci dne 3. 10. 2017

O průběhu SDZ je veden protokol.

10. Recommendation of the supervisor

Supervisor's opinion on PhD thesis of Muhammad Usman Javaid, MIT

Date: 20.5.2019

Thesis Title: **Knife Stabbing Resistance of Woven Fabrics**

Doctoral Scholar: Muhammad Usman Javaid

The thesis titled „Knife Stabbing Resistance of Woven Fabrics" submitted by Muhammad Usman Javaid, MIT fulfils the objectives mentioned in this thesis. The work is comprehensive and shows his analytical ability to design the research and to evaluate the theoretical and experimental results. He has published work from his dissertation, in reputed impact factor journals and has presented at various occasions.

This work includes the analysis of isotropy of knife stabbing of single and multiple sheets fabrics. Para-Aramid woven fabric is studied in this work, whose surface friction is modified by treating it with SiO_2, TiO_2 and Ozone. Stabbing is complex phenomenon due to the involvement of many variables. Many experiments are performed to measure the response of various fabrics in five cutting directions. Multiple sheet stacks are also studied for theirorientation at a specific stacking angle. Quasi-static and dynamic stab resistence is measured. Various fabrics are also characterized for their surface topology, comfort, physical, and mechanical properties.

The focus of the study is the dynamic and quasi-static stab resistance of fabrics at differentcutting directions and stacking of sheets at different orientation directions. Results reveal that when mechanical properties of warp and weft are significantly different the knife stabbing direction may become significant. The coefficient of friction between yarns and orientation o fangle of sheets has a direct impact on the fabrics' response. On higher friction and 45° orientation of sheets, the knife stabbing direction becomes insignificant. Furthermore, significantly higher response of quasi-static and dynamic stab resistence was observed that increased by more than 200%. It was deduced to distribute the penetration energy in various directions and clogs the knife penetration.

Formally, work is right, taken over parts of the text or images are properly cited and all sources of literature are in agreement with arranged rules. Plagiarism checking on 20.5. 2019 prove no relevant similarity to other work

This thesis is well written, and the quality of the graphs and tables is very good, and they are well presented. The overal quality of the thesis is very good, and I recommend it for defence.

.

Liberec, 20.5.2019

Ing. Jana Salačová, PhD.

11. Opponents' reviews

ČESKÉ VYSOKÉ UČENÍ TECHNICKÉ V PRAZE
Fakulta stavební
oddělení pro vědu a výzkum
Thákurova 7, 166 29 Praha 6
e–mail: obhajoby@fsv.cvut.cz tel.: 224 358 736

Posudek disertační práce

Uchazeč Muhamad Usman Javaid

Název disertační práce Knife stabbing resistance of woven fabrics

Studijní obor Textile Engineering

Školitel Ing. Jana Salačová, Ph.D.

Oponent Prof. Ing. Michal Šejnoha, Ph.D., DSc.

e-mail sejnom@fsv.cvut.cz

Aktuálnost tématu disertační práce

komentář: Scientific relevance of the submitted work

The present thesis is focused on the applicability of Aramid fiber based woven fabrics to provide protection against knife stabbing. Unlike ballistic protection armor, which has been at the engineering forefront for many years, the protection armor against sharp objects such as knifes has received less attention. There is no doubt that personal protection against such attacks plays an important role and as such the selected topic is up to date and certainly deserves attention.

☐ vynikající	☒ nadprůměrný	☐ průměrný	☐ podprůměrný	☐ slabý

Splnění cílů disertační práce

komentář: Goals of the work and their achievements
The main research objectives are clearly stated in Chapter 2. They arise from a literature survey given in Chapter 1 and particularly from the state of the art Chapter 3, which in my opinion should be part of the introductory section thus preceding Chapter 2. One may identify two principal research directions aiming (1) at improving the yarn internal friction by suitably modifying the fiber surface while not reducing the comfort properties and (2) at investigating the influence of stabbing angle with the goal of providing the most optimal layup of several fabric layers. It is clear from the overall summary provided in Chapter 6 and in particular from Chapter 5 presenting a thorough discussion on the results of extensive experimental program that all goals were successfully achieved.

☐ vynikající	☒ nadprůměrný	☐ průměrný	☐ podprůměrný	☐ slabý

Metody a postupy řešení

komentář: Treatment of the topic - methodical and conceptual approach

The methodical and conceptual approach is described in Chapter 4 presenting individual approaches to the fabric surface treatment as well as the experimental program. For the sake of clarity I would split this chapter into separate chapters combining the material section and surface treatment in one while presenting the actual experimental program devoted to the stabbing resistance measurement in a separate chapter. It might be the lack of my knowledge, but I found some parts a bit unclear. The following items might be addressed during presentation:

1. Section 4.2.2.2 - please explain how the strain of each yarn before rupture was measured.

2. Section 4.2.2.3 - it is not clear to me with respect to what direction the KPA was measured

when assuming 8 sheets in Fig. 20(c) with 45 stacking sequence.

3. Section 4.2.5.3 - it is not clear to me how the bending experiment was performed for the fabric. Neither the sample size is mentioned nor is the measurement of bending angle. The force unit [gf] is also not a standard force unit. Please provide the relation to [N].

☐ vynikající	☒ nadprůměrný	☐ průměrný	☐ podprůměrný	☐ slabý

Výsledky disertace - konkrétní přínosy disertanta

komentář: Thesis results - author's specific contribution

The principal outcomes of the theses can be extracted from Chapters 5 and 6. The author clearly identified the most optimal treatment of fabric surface, pointed out some dead ends such as the surface modification by Titanium dioxide and thoroughly described the influence of stabbing angle on the stabbing resistance. Unfortunately, similar to Chapter 4, there are some issues which need some explanation. These include:

1. Table 10 – what is the reason for reducing the thickness in treated fabrics compared to a Neat fabric? Are these fabrics stretched during treatment? This might certainly have some impact, e.g. on bending rigidity. Please make a comment on that.

2. Table 11 – what type of fabric these results refer to? There is no comparison between treated and untreated fabrics.

3. Figure 33 – it is not clear what KPA the plotted results refer to.

4. Figure 35 – it is not clear to what percentage of WG the results refer to.

5. Figure 36 – I suppose the notation 2ZS4 refers to the last read square only. How about 20% WG, does that mean 2ZS3? Please explain.

6. Section 5.12. Do I understand correctly that the effect of stacking sequence has been examined for the untreated fabric only? Why not for the treated fabric as well. That I would found more important. Or perhaps I am missing something. Please make a breaf comment on that.

☐ vynikající	☒ nadprůměrný	☐ průměrný	☐ podprůměrný	☐ slabý

Význam pro praxi a pro rozvoj vědního oboru

komentář: Extent of new knowledge and contribution to the practice

The thesis ceratinly shed light on a number of specific issues concerning the protection armor againts sharp objects. But I am not an expert in this field so I suggest the author to give, during the thesis defense, his own opinion on a potential applicability of the proposed surface treatment in practice.

☐ vynikající	☐ nadprůměrný	☐ průměrný	☐ podprůměrný	☐ slabý

Formální úprava disertační práce a její jazyková úroveň

komentář: Organization of the work and overall comprehensiveness

The thesis are written in good English with only few grammatical errors. It is well structured and easy to follow. The only source of criticism is associated, as already mentioned, with insufficient explanation of some procedures, variables or figures. The author should put more attention to that when extracting a journal paper from the presented results. But even this drawback does not reduce significantly the thesis high standard.

☐ vynikající	☒ nadprůměrný	☐ průměrný	☐ podprůměrný	☐ slabý

Připomínky

Comments:
Apart from comments raised already in the review sections "Treatment of the topic" and "Thesis results" the following questions might be addressed in more details:

1. Can you please comment on a relatively high variability in bending rigidity observed in Fig. 28 for Neat fabric in comparison to treated fabrics?
2. Section 5.12.5 - please make a brief comment on the last sentence. In particular, what would be your approach to the optimum design?
3. Section 5.13 - please make a brief comment on the last sentence. In case of QSKPR you promote the 450 angle as most efficient in comparison to other SAs. So how is this related to the requirement of a small stacking angle in case DSR? How about zero degree angle?
4. Should we be concerned with material aging, i.e. degradation of properties of treated fabrics with time? How about the effect of temperature?

Závěrečné zhodnocení disertace

Final statement:

Based on the submitted review, consisting of an assessment of the scientific relevance, fulfillment of the goals of the work, the quality of treatment of the topic and the extent of new knowledge, it is concluded that this work meets high quality standards.

As it complies with the requirements for a Ph.D. work, I recommend the thesis for further defense and if successful to appoint Mr. M.U. Javaid the title

doctor (Ph.D.)

Doporučuji po úspěšné obhajobě disertační práce udělení titulu Ph.D. *ano* ☒ *ne* ☐

Datum: 24.7.2019

Podpis oponenta: ....

Review

Dissertation of

Muhammad Usman Javaid

called

Knife Stabbing Resistance of Woven Fabrics

Liberec, 29th July 2019 *written by: doc. Ing. Lukáš Čapek, Ph.D.*

1. Introduction

The thesis has 103 pages comprising graphs, figures and tables. The appendix contains the bibliography and author´s scientific articles aiming to the topic of the work. The work has six chapters that contains introduction following by independent research topics. The principle goal of the work is to get a knowledge how woven fabric behave against change orientation of knife stab and according to this knowledge increase the resistance properties of selected woven fabric by changing the friction behaviour of individual fibres.

2. Comments to originality and aims of the work

The stab resistance of different textile fabric is a current topic with importance regarding the increasing number of stab attacks worldwide. From the scientific point of view, the topic is still open with many unsolved tasks. The aims of the work are well described in the chapter two. However, the scientific hypotheses are missing. My opinion is that the scientific work should have hypotheses. If not, it decreases the work to a general engineering issues.

3. Comments to the state of the art and methods used in the work

To my opinion the state of the art is insufficient. There are much more articles dealing with stab resistance (AND/OR) textile fabric following standard scientific article websites. Some of them are marginal, but some of them are completely focused on the same topic. Namely the PhD thesis of Priscilla Reiners focused on Investigation about the stab resistance of textile structures, methods for their testing and improvements could not be skipped in this work.

The work flow of used methods is well described in figure 13. I really appreciated it. The standardized tests are well described and there is no need for comments. On the other hand, the individual yarn cutting resistance experiment is not described well. It is not clear how the experiment was done. The figure 22 is misleading and there is no description what letters in the figure mean.

Questions to author:

1) Explain the individual yarn cutting resistance experiment. Mainly focus how you get outcomes from this experiment (force and energy).
2) Can you explain why you provided the air permeability and surface feel properties measurement? How these experiments are linked to your topic?

4. Comments to results

It is evident that the author provided a large number of experiments. Unfortunately, regarding the number of experiments, the results are not well described.

Questions and comments to this section:

1) Why you start your results with your last experiment?
2) Can you explain why there is so high scatter in your results for neat fabrics and so low for treated one (Fig. 28)?
3) Figure 41 – what means best of various samples?
4) Page 59 – "….QSKPR increase linearly with the increase in amount of SiO_2…". I cannot see it from fig. 40. Can you prove it?
5) Page 62 – why you make conclusion from experiment on sketch? How can one believe it? Can you prove it on images gained from experiment? Is the knife really sliding on the surface of the fabrics?
6) Page 63 – what do you mean by the expression "plastic deformation"?
7) Page 63 – what is the meaning of sentence "The ultimate tensile strength of yarns removed from different fabrics…"?
8) Page 68 – figure 47 – units on vertical axis is missing.
9) Regarding comment 1 above in methods, can you explain the results in 5.9 more deeply?

5. Overall decision

I invite the author to answer my questions during the defence of the work.

I recommend the work for defence

(Doporučuji práci k obhajobě)

doc. Ing. Lukáš Čapek, Ph.D., v.r.

Technická Univerzita v Liberci